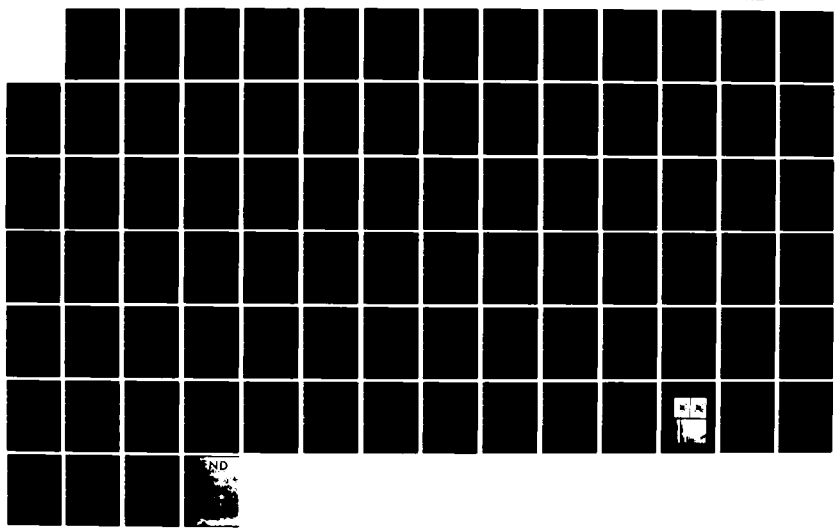


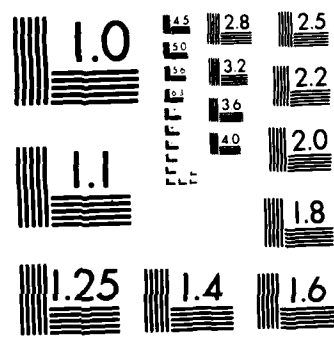
AD-A129 488 ELECTRICALLY CONDUCTING POLYMERS(U) IBM RESEARCH LAB 1/1  
SAN JOSE CA W D GILL ET AL. 07 APR 83 TR-8  
N00014-80-C-0779

UNCLASSIFIED

F/G 7/3 NL



END



MICROCOPY RESOLUTION TEST CHART  
NATIONAL BUREAU OF STANDARDS-1963-A

ADA129488

OFFICE OF NAVAL RESEARCH

Contract N00014-80-C-0779

Technical Report No. 8

Electrically Conducting Polymers

by

W. D. Gill, T. C. Clarke, and G. B. Street

Prepared for Publication

in

Electrical Properties of Polymers

(A. M. Herman, ed.)

IBM Research Laboratory  
5600 Cottle Rd.  
San Jose, CA 95193

April 7, 1983

Reproduction in whole or in part is permitted for  
any purpose of the United States Government

This Document has been approved for public release  
and sale; its distribution is unlimited

REPRODUCED BY  
NATIONAL TECHNICAL  
INFORMATION SERVICE  
U.S. DEPARTMENT OF COMMERCE  
SPRINGFIELD, VA 22161

# Research Report

ELECTRICALLY CONDUCTING POLYMERS

W. D. Gill  
T. C. Clarke  
G. B. Street

IBM Research Laboratory  
San Jose, California 95193

**IBM**

Research Division  
Yorktown Heights, New York • San Jose, California • Zurich, Switzerland

83 04 26 011

Copies may be requested from:  
IBM Thomas J. Watson Research Center  
Distribution Services  
Post Office Box 218  
Yorktown Heights, New York 10598

RJ 3838 (43805) 3/25/83  
Chemistry

## **ELECTRICALLY CONDUCTING POLYMERS**

**W. D. Gill  
T. C. Clarke  
G. B. Street**

**IBM Research Laboratory  
San Jose, California 95193**

### **ABSTRACT**

This paper reviews the present state of the field of conducting polymers.

## I. INTRODUCTION

In parallel with developments in the field of quasi one-dimensional organic metals [1-3], intense interest in other possibly low-dimensional conducting systems has led to investigation of a number of polymer systems with high conductivity potential. The obvious chemical and structural anisotropy of polymers immediately suggested that a conducting polymer might have the highly anisotropic electrical properties seen in quasi one-dimensional conducting crystals such as KCP [2] and TTF-TCNQ [1,3]. Polycrystalline compactations of polythiazyl  $(SN)_x$  were known to be highly conducting from the work of Chapman *et al.* [4], who had concluded that the material was a semiconductor. In 1973 Walatka *et al.* [5] reported results of electrical measurements on crystals of  $(SN)_x$ . The metallic conductivity along the polymer chain axis observed by these authors stimulated extensive research into the properties of the material. With the discovery of superconductivity in  $(SN)_x$  crystals by Greene, Street and Suter [6] the investigation of  $(SN)_x$  and the search for other highly conducting polymers rapidly developed.

Attempts to synthesize chemical analogs of  $(SN)_x$  were disappointing, but modification of the electronic properties of  $(SN)_x$  by reaction with oxidants led to the interesting halogen modifications of  $(SN)_x$  by Bernard *et al.* [7] and independently by Street *et al.* [8,9] and Aktar *et al.* [10,11]. The brominated  $(SN)_x$  modification  $(SNBr_{0.4})_x$  with conductivity of  $2-3 \times 10^4 \text{ ohm}^{-1}\text{-cm}^{-1}$  remains the highest conductivity polymer measured to date.

The next advance in this field was the discovery of organic polymer systems with metallic properties. For many years the properties of long chain polyenes had been

theoretically investigated as potential semiconductors [12]. However, the longest polyene chains were less than 20 units long. As far back as 1958 polymerization of acetylene to essentially infinite polyene chains had been successfully carried out in the presence of a Ziegler catalyst [13]. The product of these early reactions was a fine powder of polyacetylene, whose powder compaction conductivity was found to increase substantially on exposure to a wide range of oxidizing molecules [14]. In 1974, Ito *et al.* [15] discovered that by exposing high concentrations of the Ziegler catalyst to a relatively high pressure of acetylene gas, polyacetylene films were formed. Then in collaboration with MacDiarmid and Heeger at the University of Pennsylvania doping experiments on polyacetylene films with various oxidants resulted in conductivities as high as  $1000 \text{ ohm}^{-1}\text{-cm}^{-1}$  [16]. This discovery has stimulated extensive investigation of polyacetylene and other organic polymers in many laboratories with the result that a number of organic polymers with metallic-like conductivities have now been discovered.

Our purpose in this chapter is to describe some of the physics and chemistry of these highly conducting polymer systems ranging from the inorganic  $(\text{SN})_x^n$  to organic materials such as  $(\text{CH})_x^n$ , polypyrrole and the polyphenylenes [17]. It would be very difficult in a single chapter to adequately review the already extensive literature on these materials. Instead we hope to present a coherent overview of the current status of highly conductive polymers and to refer the interested reader to several review articles for a more extensive survey of the literature.

## II. POLYTHIAZYL (SN)<sub>x</sub>

### A. Synthesis of (SN)<sub>x</sub>

#### 1. (SN)<sub>x</sub>, CRYSTAL GROWTH, FILM GROWTH AND STABILITY

In his paper in 1910, Burt [18] true to his middlename, Playfair, acknowledged that (SN)<sub>x</sub> was first prepared by Davis. Burt prepared both films and crystals of (SN)<sub>x</sub> by the thermal pyrolysis of S<sub>4</sub>N<sub>4</sub> in the course of trying to remove excess sulfur from the S<sub>4</sub>N<sub>4</sub> by passing its vapors over silver wool. The silver wool acts as a catalyst [19] in the conversion of S<sub>4</sub>N<sub>4</sub> to S<sub>2</sub>N<sub>2</sub> [20]. As the crystal structure of S<sub>2</sub>N<sub>2</sub> reveals [21] the square planar S<sub>2</sub>N<sub>2</sub> molecules are ideally arranged for a solid state polymerization to (SN)<sub>x</sub>. The mechanism of the solid state reaction has been studied by Baughman *et al.* [22]. Burt's paper provides the basis of the techniques used today to prepare the (SN)<sub>x</sub> crystals which have been used in the investigation of its electrical properties. All of these techniques [23-25] emphasize the importance of the purity of the intermediate S<sub>2</sub>N<sub>2</sub> crystals and careful temperature control during their slow solid state polymerization. Labes *et al.* [26,27] have also investigated crystal growth techniques involving photoinitiation of polymerization of solution grown S<sub>2</sub>N<sub>2</sub> crystals.

Films of (SN)<sub>x</sub> have also been investigated extensively. They have been prepared by two techniques, pyrolysis of S<sub>4</sub>N<sub>4</sub> and direct heating of (SN)<sub>x</sub> [28-30]. Films in which the (SN)<sub>x</sub> chain direction is ordered can be prepared by deposition on mylar treated to provide a series of parallel scratches on the surface [31]. The vapors above both (SN)<sub>x</sub> and S<sub>4</sub>N<sub>4</sub> have been studied in detail [32,33] and they contain species which would contaminate the resulting films. This contamination can be minimized and the properties of the films modified by careful control of the substrate temperature [34,35]. Smith *et al.* [36] and Saalfeld *et al.* [37] concluded that the main component of the vapor from (SN)<sub>x</sub>

was an  $(SN)_4$  bent chain species. Such a structure would have an electric dipole moment, which is not consistent with the results of molecular beam electric deflection analysis [38]. Iqbal *et al.* [39] have interpreted IR spectra of  $(SN)_x$  films deposited at low temperatures as evidence for linear  $(SN)_x$  oligomers.

Though both films and crystals of  $(SN)_x$  are stable indefinitely in inert atmospheres they decompose in air [40]. This decomposition is observed most readily for thin films and is also frequently first observed on those crystal faces where the chains terminate. The stability of the films and crystals is negatively affected by the presence of unpolymerized  $S_2N_2$  as well as other impurities. Nuclear relaxation studies [41] have shown that  $(SN)_x$  adsorbs water quite rapidly, resulting in the presence of high hydrogen concentration in the material. Seel *et al.* [42] have calculated the effects of hydrogen on the density of states in  $(SN)_x$ . However, no experimental correlations exist between the physical properties of  $(SN)_x$  and its hydrogen content either from adsorbed water or other sources.

### B. Structure of $(SN)_x$

On the basis of its complete insolubility, Burt in 1910 characterized  $(SN)_x$  as a polymer [18]; however, it was not until 1956 that Goehring and Voigt first investigated its structure and suggested a zig-zag geometry for the chain [43]. Doullard [44] showed that this geometry was incorrect and advanced what has proved to be essentially the correct chain structure. A preliminary crystal structure obtained from electron diffraction [45] using this chain geometry was later refined by X-ray diffraction [21] and confirmed by neutron diffraction techniques [46]. This structure is shown in Figure 1. The unit cell contains two almost flat chains, which are centrosymmetrically related but translationally

inequivalent. These inequivalent chains alternate along the c-axis whereas equivalent chains are adjacent along the a-axis. The chains all lie in the  $10\bar{2}$  plane where equivalent chains alternate. This  $10\bar{2}$  plane is an easy cleavage plane. The shortest interchain bonds are tabulated in Table 1. Comparison of these bond lengths with the corresponding van der Waals diameters suggests that the interaction between the chains are weak relative to the bonding within the chains.

Studies of the vibrational spectra of  $(SN)_x$  using both Raman and IR techniques [47-50] have also given useful insight into the relative strengths of the intrachain and interchain bonding. In general these data confirm the conclusions from other measurements that  $(SN)_x$  has a high degree of structural anisotropy. The intrachain force constants are significantly larger than the interchain force constants.

### C. Electronic Properties

#### 1. BAND STRUCTURE

The intrinsic electronic properties of any crystalline solid, i.e., whether it is a metal, semimetal, semiconductor or insulator, are determined by its electronic band structure. Once the crystal structure has been completely determined, this band structure can in principle be calculated exactly. However, due to the large number of electrons in the unit cells of polymeric conductors (44 electrons in the case of  $(SN)_x$ ) various approximations are necessary. A large number of band structure calculations for  $(SN)_x$  have been made ranging from relatively simple one-dimensional extended Hückle tight-binding methods to a complete three-dimensional orthogonalized plane wave calculation [51].

The  $(SN)_x$  structure contains two chains per unit cell, each with two SN pairs related by a screw axis symmetry. Simple one-dimensional band calculations for this structure [52] predict a half-filled conduction band with a degeneracy at the Brillouin zone boundary. This degeneracy should be split by a Peierls distortion resulting in an insulating state for the system. Experimentally it was known that  $(SN)_x$  was metallic and did not undergo a Peierls transition even at very low temperature [5]. It was therefore necessary to include interchain interactions which could stabilize the structure against such a Peierls distortion. A variety of three-dimensional calculations have been made which show that quite extensive interchain coupling in  $(SN)_x$  stabilizes the metallic state; thus  $(SN)_x$  must be regarded as a highly anisotropic conductor instead of a quasi one-dimensional metal. As we will discuss below these calculations verified the conclusions on dimensionality already experimentally established from optical anisotropy [53] and electron energy loss measurements [54].

The three-dimensional OPW calculation of Rudge and Grant [55] gives the most complete picture of the band structure (Figure 2) and Fermi surface of  $(SN)_x$ . The Fermi level crosses the overlapping bands in the chain direction ( $\Gamma$  to Z) and in the perpendicular direction (Z to E), resulting in electron pockets at Z and hole pockets at E. Thus, the calculations show that  $(SN)_x$  is a semimetal, but perhaps more importantly they also demonstrate that although  $(SN)_x$  is strongly anisotropic, it should not be regarded as a quasi one-dimensional conductor. The expected degree of anisotropy has been estimated from the OPW band structure by Grant *et al.* [56], who derived the plasma tensor anisotropy by suitable integration over the Fermi surface. The magnitude of the principal axes for the plasma tensor is in the ratios 1:0.13:0.09 in the  $b:(\bar{1}02)_\parallel:(\bar{1}02)_\perp$  directions, in reasonable agreement with experiments discussed below.

## 2. NORMAL CONDUCTIVITY AND SUPERCONDUCTIVITY

The transport measurements of Walatka *et al.* [5] in 1973 on  $(SN)_x$  crystals stimulated the recent interest in this material. Conductivity and thermoelectric power measurements strongly suggested that  $(SN)_x$  was metallic to 4.2K in the direction parallel to the  $(SN)_x$  chains in the crystal structure. Strong anisotropy was observed for conductivity parallel and perpendicular to the fiber axis of the crystals, which coincides with the  $(SN)_x$  chain axis. This anisotropy led to early speculation that  $(SN)_x$  was a quasi one-dimensional conductor. However, the persistence of metallic conductivity to very low temperatures, where a Peierls transition to the insulating state would be expected for a one-dimensional system, suggested that the fibrous nature of  $(SN)_x$  crystals might be dominating the observed conductivity anisotropy.

In 1975, Greene *et al.* [6] discovered superconductivity in  $(SN)_x$  with  $T_c=0.3\text{K}$ . This observation, which dramatically verified the metallic properties of  $(SN)_x$ , was also the first observation of superconductivity in a polymer and the first observation of superconductivity at ambient pressure in a material containing no metallic elements. The superconductivity experiments suggest that  $(SN)_x$  is a bulk type II superconductor but that crystal perfection strongly affects the superconductivity.

The effects of improved crystal perfection on the conductivity properties is shown in Figure 3 [57]. The maximum conductivity increased from  $1000 \Omega^{-1}\text{cm}^{-1}$  to about  $4000 \Omega^{-1}\text{cm}^{-1}$  while the resistivity ratio  $\rho_{RT}/\rho_{4\text{K}}$  increased from about 3 to 250. The superconductivity transition temperature  $T_c$  also increased from 0.26K to 0.35K. The quadratic dependence of resistivity on temperature observed with the best crystals suggested to Chiang *et al.* [58] that the usual electron-phonon scattering processes are not

dominant in  $(SN)_x$  but that electron-electron Umklapp scattering between electron and hole pockets of the Fermi surface is dominant.

The unusual pressure dependence of normal conductivity should be mentioned here since it provides additional support for the electron-electron scattering process and also gives some insight into the transport and optical properties of brominated  $(SN)_x$  described in a later section. Under hydrostatic pressure the increase in normal conductivity is more than an order of magnitude greater than expected from lattice stiffening effects on electron-phonon scattering processes [59]. However, electron-electron scattering can be expected to be extremely pressure sensitive through its dependence on details of the Fermi surface. Consideration of the effects of hydrostatic pressure on the band structure indicate that the electron pocket may be shifted from the Brillouin zone center thus reducing the electron-hole scattering probability with a resultant increase in conductivity [65].

Early attempts to observe a Meissner effect in  $(SN)_x$  crystals were unsuccessful [61] leaving some doubt as to whether the observed superconductivity was a bulk effect. However, a broad hump in the specific heat indicative of the expected BCS anomaly was observed [62]. More recently the Meissner effect has been observed [63,64] verifying the model of  $(SN)_x$  as a bulk, weakly coupled filamentary Type II superconductor. A number of interesting problems related to superconductivity in  $(SN)_x$  still need to be resolved. These include the pressure dependence of  $T_c$ , which increases strongly with pressure to about 8 Kbar where a sudden decrease in  $T_c$  apparently signals a change in phase [65,66]; the absence of superconductivity in  $(SN)_x$  films [67-69]; and the absence of a superconducting gap in tunneling experiments [70]. Full understanding of the temperature

dependence of the critical magnetic field and its strong anisotropy [71] also provides interesting challenges. The explanation of the very broad superconducting transition width as fluctuations of one-dimensional superconductivity [72] is intriguing in view of the results observed in  $(\text{SNBr}_{0.4})_x$  described below.

### 3. OPTICAL PROPERTIES

The optical properties of  $(\text{SN})_x$  crystals have been measured by several groups [53,73] and have played an important role in understanding the intrinsic properties. Optical reflectivity with the E-vector of the incident light parallel to the chain axis (b-axis) shows a steep, metallic reflectance edge which can be analyzed using the Drude model, yielding a plasma frequency  $\hbar\nu_p = 6.9 \text{ eV}$  and a scattering time  $\tau = 2.6 \times 10^{-15} \text{ sec}$  [53]. The optical conductivity derived from these measurements,  $\sigma_{\text{opt}} = 2/4 = 2.5 \times 10^4 \Omega^{-1} \text{ cm}^{-1}$ , is about an order of magnitude greater than the measured DC conductivity. With the E-vector perpendicular to the b-axis a much weaker structure is observed in reflectivity and is interpreted to be a strongly damped plasma edge at  $\hbar\nu_p = 2.4 \text{ eV}$  with  $\tau = 3 \times 10^{-16} \text{ sec}$ . The observation of this perpendicular reflectivity edge was the first experimental evidence that  $(\text{SN})_x$ , although strongly anisotropic, should not be regarded as a quasi one-dimensional metal. This conclusion is also supported by electron energy loss experiments [54] and by magnetoresistance anisotropy [74] and is in good agreement with the three-dimensional OPW band structure calculations [55,56].

### 4. OTHER PHYSICAL PROPERTIES

A broad range of experimental techniques have been applied to  $(\text{SN})_x$  to measure both its lattice and electronic properties. These experiments include specific heat [75], inelastic neutron scattering [76], IR reflectance, Raman scattering [47,48], X-ray [77] and

ultraviolet photoemission [78], magnetoresistance [74,79,80], Hall effect [80] and junction properties [81,82]. Space permits only a very brief review of these experiments which, however, demonstrate some very interesting and important properties of this material.

From the electronic contribution to the specific heat, Harper *et al.* [75] obtain a value for the Fermi level density of states of 0.14 states/eV-spin-molecule in excellent agreement with band structure predictions. The temperature dependence of the lattice contribution to the specific heat is characteristic of a solid with quasi one-dimensional binding forces. From IR, Raman and neutron scattering results, Stoltz *et al.* [47] estimate that the interchain force constants are about ten times smaller than the intrachain force constants.

The X-ray photoemission [77] and uv-photoemission [78] results give valence band densities of states which again agree very well with band structure predictions (see Figure 2). A value of about 0.5 electrons transferred from S to N is obtained from these experiments consistent with theoretical predictions.

Several measurements of the galvanomagnetic properties of  $(\text{SN})_x$  crystals have been reported. Beyer *et al.* [74] measured the magnetoresistance anisotropy at 4.2K and compared it with the anisotropy derived from the calculated plasma tensor of Grant *et al.* [56]. A negative magnetoresistance dominated the measurements at low magnetic fields. At higher fields a quadratic positive magnetoresistance was observed with a parallel to transverse mobility anisotropy ratio of 3.1, in reasonable agreement with calculated value of 5.7. The b-axis mobilities are about  $600 \text{ cm}^2/\text{V}\cdot\text{sec}$  and  $400 \text{ cm}^2/\text{V}\cdot\text{sec}$  for holes and electrons, respectively. A scattering time of  $1.5 \times 10^{-13} \text{ sec}$  was obtained

corresponding to a mean free path of  $\sim 700\text{\AA}$  along the b-axis. The Hall effect could not be observed in these experiments. Kahlert and Seeger [80] have reported magnetoresistance on samples with exceptionally high ratios of  $\sigma_{4K}/\sigma_{300K}$ . No negative component of magnetoresistance was observed until after severe bending of the crystals, suggesting that this anomalous effect is connected with defects. Kaneto *et al.* [79] attribute the negative magnetoresistance to spin-dependent scattering at chain breaks or defects with localized spins. Kahlert and Seeger [80] have observed the Hall effect for an  $(\text{SN})_x$  crystal, from which a value of the effective carrier density  $n_{\text{eff}} = 3.2 \times 10^{21} \text{ cm}^{-3}$  was obtained in excellent agreement with band structure results.

Junction properties measured by Scranton *et al.* [81] have shown the interesting result that  $(\text{SN})_x$  is more electronegative than gold, producing large Schottky barriers on contact with n-type semiconductors. A practical utilization of this property in Schottky Barrier solar cells has been investigated by Cohen and Harris [82].

### 5. $(\text{SN})_x$ FILMS

The previous discussion has been concerned with the properties of  $(\text{SN})_x$  crystals. However, thin films of  $(\text{SN})_x$  have interesting optical properties and a wide range of electrical properties.

Although the polycrystalline films are usually disordered, films with highly anisotropic optical properties were obtained by Bright *et al.* [31] from depositions on stretched films and especially on mylar films which had been lightly abraded or rubbed in one direction. Films deposited on these substrates have almost complete alignment of the  $(\text{SN})_x$  crystallites with the polymer chain axes (b-axis) in the direction of the stretching or

abrasion. This crystallite alignment results in strongly anisotropic optical and transport properties. The optical anisotropy has interesting potential application as a polarizer in the visible and near infrared.

The electrical properties of  $(SN)_x$  films have been studied extensively [67,68,29,35]. The conductivity is dominated by interparticle barrier effects resulting in an activated-like temperature dependence instead of metallic-like behavior. The effects of substrate temperature on conductivity, thermoelectric power, Hall effect and magnetoresistance have been investigated by Beyer *et al.* [68,35]. Thermoelectric power and conductivity results shown in Figure 4 indicate that the metallic transport properties of  $(SN)_x$  crystals are approached as the substrate temperature is increased. However, superconductivity was not observed even in the most metallic of these films. A model for the film transport results suggests the existence of a gap in the density of states correlated with  $(SN)_x$  chain length [35]. Such a gap might also explain the absence of superconductivity in  $(SN)_x$  films [68].

### III. CHEMICAL MODIFICATIONS OF $(SN)_x$

#### A. General Survey

The discovery of superconductivity in crystals of  $(SN)_x$  motivated intensive efforts in several laboratories to synthesize analogous compounds. Much of this work was focussed on efforts to produce  $(SeN)_x$  from the known compound  $Se_4N_4$  by routes similar to those described for conversion of  $S_4N_4$  to  $(SN)_x$  [57]. These efforts have not been successful. Similarly unsuccessful attempts have also been made to produce  $(SCN)_x$  [83]. Oligomeric analogs of  $(SN)_x$  such as 1,9-diaryl-pentasulfurtetrinitride [84] have been prepared but they showed no evidence of conductivity despite the fact that there was an

increasing red shift of the uv-visible absorption with increasing chain length indicating extensive electron delocalization along the chain. Attempts to make even longer chain oligomers were not successful.

## B. Halogen Modifications

### 1. PREPARATION

The  $(SN)_x$  chain and crystal structures were shown above in Figure 1. The unit cell of  $(SN)_x$  contains two, almost flat, translationally inequivalent, centrosymmetrically related  $(SN)_x$  chains. These two inequivalent chains alternate along the c-axis, whereas equivalent chains are adjacent along the a-axis. The chains all lie in the  $10\bar{2}$  plane where equivalent chains alternate. The ready cleavage which takes place at these  $10\bar{2}$  planes suggest the possibility of intercalating various molecules between them. In 1976 Bernard *et al.* [7] reported the formation of an intercalation compound of  $(SN)_x$  and bromine. Independently Street and Gill [8,9] surveyed a large number of potential intercalates and found that the halogens  $Br_2$ ,  $I_2$ ,  $ICl$  and  $IBr$  all increased the conductivity of  $(SN)_x$ . The bromine derivatives have been more extensively studied because they show the highest conductivity.

The simplest preparative technique for brominating  $(SN)_x$  is exposure to dry bromine vapor. On exposure  $(SN)_x$  crystals change color from gold to blue-black and expand in directions perpendicular to the chain axis. Exposure to the vapor pressure of bromine at room temperature leads to a composition  $(SNBr_{0.5})_x$  which on pumping in vacuum ( $10^{-5}$  Torr) at room temperature for one hour gives a final composition of  $(SNBr_{0.4})_x$ . At this composition the crystal has expanded by approximately 50% in volume perpendicular to the chain axis. The flotation density increases from  $2.32 \text{ g/cm}^3$

to 2.65 g/cm<sup>3</sup>. Virtually any composition of lower bromine content can be obtained by heating a sample of  $(SNBr_{0.4})_x$  in vacuum for various periods of time. However, the  $(SNBr_{0.4})_x$  composition appears to have the best electrical properties and has been most extensively studied. It is important to brominate with bromine vapor because  $(SN)_x$  reacts with liquid bromine yielding significant amounts of a side product  $S_4N_3Br_3$  [85].

A different preparative route involves direct bromination of the  $(SN)_x$  precursor molecule  $S_4N_4$  [86,87]. Exposure to bromine vapor causes  $S_4N_4$  crystals to turn black and expand rapidly destroying their external habit. After removal of free bromine the remaining, conductive black powder has the composition  $(SNBr_{0.4})_x$ . IR [88], Raman [89], thermal analysis [88] and mass spectrometry [90] all indicate that this material is the same as that obtained by bromination of  $(SN)_x$  crystals; however, it is even more structurally disordered. The mechanism of this ring opening reaction is unknown. ICl and IBr vapor also react readily with  $S_4N_4$  to form conducting solids [86,87,91].

Considerable effort has gone into studies of the molecular nature of the intercalated halogens in  $(SN)_x$  derivatives. In graphite, bromine is known to be present in the form of weakly ionized  $Br_2^-$  [92]. However, in  $(SN)_x$  Raman spectroscopy indicates a much more complex situation [89,50]. Two strong Raman fundamentals are observed at 150 cm<sup>-1</sup> and 230 cm<sup>-1</sup>. The first band has been assigned without ambiguity to the symmetric stretch of the tribromide ion,  $Br_3^-$ . The band at 230 cm<sup>-1</sup> can be assigned to the asymmetric stretch of the same  $Br_3^-$  ion or to the stretching frequency of  $Br_2$  downshifted from its 325 cm<sup>-1</sup> frequency in the gas phase by its strong association with the  $(SN)_x$  lattice. Macklin *et al.* [93] examined the IR absorption of brominated  $(SN)_x$  and found no evidence for the 230 cm<sup>-1</sup> peak which would be expected to be IR active for the

asymmetric stretch of a linear  $\text{Br}_3^-$  ion. On this basis it is concluded that both  $\text{Br}_2$  and  $\text{Br}_3^-$  molecular species are present in brominated  $(\text{SN})_x$ . From the polarization dependence of the Raman peaks the  $\text{Br}_2$  and  $\text{Br}_3^-$  appear to be oriented with their axes parallel to the  $(\text{SN})_x$  chains. Extended X-ray Absorption Fine Structure (EXAFS) studies [94] are also consistent with this orientation and indicate that similar concentrations of  $\text{Br}_2$  and  $\text{Br}_3^-$  species are present in the  $(\text{SNBr}_{0.4})_x$  crystals. Magnetic susceptibility measurements show the absence of paramagnetic species such as  $\text{Br}_2^-$  [95].

Mass spectrometric studies of the species emanating from the surface of heated  $(\text{SNBr}_{0.4})_x$  [90,96] show an initial high concentration of  $\text{Br}_2$  which rapidly decreases and a lower concentration of  $\text{SNBr}$  which becomes the dominant volatized species after the first few hours. These results can be rationalized by assuming the bromine to be in the two molecular forms  $\text{Br}_2$  and  $\text{Br}_3^-$ .

## 2. STRUCTURE OF $(\text{SNBr}_{0.4})_x$

The incorporation of bromine into the  $(\text{SN})_x$  lattice increases the disorder and twinning so that a complete single crystal X-ray structure determination is not possible [9,54]. Data from which the mode of bromine incorporation is inferred have been obtained from electron diffraction [9], X-ray powder diffraction [7,9,50], EXAFS [94], Raman [89] and IR spectroscopy [93]. In their original experiments, Bernard *et al.* [7] concluded from X-ray powder data that only the repeat unit in the chain direction remains unchanged on bromination. This result has been confirmed from X-ray precession photographs [8,9]. Iqbal *et al.* [50] showed that as the bromine content increased,  $d(100)$

decreased and  $d(002)$  increased to an essentially common value of  $3.62\text{\AA}$ . The interplanar separation  $d(10\bar{2})$  was found to decrease.

Electron diffraction studies show patterns typical of  $(\text{SN})_x$  but with considerable streaking perpendicular to  $b^*$  indicating increased disorder and (100) twinning (Figure 5) [9]. Bromination results in a decrease in the average fiber diameter from  $\sim 70\text{\AA}$  to  $\sim 30\text{\AA}$ . Superimposed on the  $(\text{SN})_x$ -like diffraction pattern are diffuse lines at  $(0, 1/2k, 0)$  corresponding to a one-dimensional commensurate superlattice oriented along the chain axis with a repeat unit twice that of  $(\text{SN})_x$ . In addition, diffuse lines appear near  $2b/3$ ,  $2b/5$  and  $2b/7$  [97]. Diffuse X-ray scattering measurements by Comes [98] confirm these electron diffraction observations. On cooling below  $\sim 150\text{K}$  the  $2b$  superlattice lines disappear, but they reappear on warming [97]. This reversible transition is quite sharp, occurring over about a five degree temperature interval. However, the diffuse lines remain at low temperature but irreversibly weaken in intensity on heating the samples above  $100\text{C}$ . This behavior suggests that these diffuse lines are associated with the adsorbed  $\text{Br}_2$  species, which is known to evolve at these temperatures from the mass spectrometric results. The  $2b$  superlattice is believed to be associated with ordering of the linear  $\text{Br}_3^-$  ions along the  $(\text{SN})_x$  chains. The disappearance of this superlattice structure at low temperature is not understood. On the basis of Raman studies of iodinated  $(\text{CH})_x$ , Fubino *et al.* [98] have suggested that the iodine is in the form of  $\text{I}_3^-$ ,  $\text{I}_5^-$  and  $\text{I}_2$ . Attempts to understand the structure of  $\text{ICl}/(\text{SN})_x$  complexes have met with much more limited success, but both Raman- and electron-diffraction results [97] have been interpreted on the basis of un-ionized  $\text{ICl}$  adsorbed on the surface of the  $(\text{SN})_x$ .

### 3. ELECTRONIC PROPERTIES

Bromination of  $(SN)_x$  results in marked changes in optical properties, a dramatic increase of the normal conductivity, and improved superconductivity characteristics. It is particularly interesting that these improved properties can be attributed to subtle changes in  $(SN)_x$  characteristics due to electronic effects of the intercalate. The electronic properties of brominated  $(SN)_x$  suggest that this material can, to first order, be regarded as  $(SN)_x$  whose transport properties have been optimized by the bromine interaction.

The conductivity of  $(SN)_x$  films and crystals exposed to bromine to form  $(SNBr_{0.4})_x$  is increased by an order of magnitude so that  $\sigma_1 = 2 \text{ to } 4 \times 10^4 \Omega^{-1} \text{cm}^{-1}$  at 300K [8-11]. On cooling, the temperature dependence is weaker than the  $T^2$  dependence of  $(SN)_x$ . Thermoelectric power measurements [9] show a change in sign on bromination from negative to small positive values consistent with bromine acting as an acceptor. The conductivity perpendicular to the  $(SNBr_{0.4})_x$  fibers, unlike that of  $(SN)_x$ , is metallic to 3K, below which it is temperature independent [9]. This behavior suggests that  $(SNBr_{0.4})_x$  is more three dimensional, i.e., the fibers are better coupled than  $(SN)_x$  itself. In contrast to  $(SN)_x$ , where  $\sigma$  increases dramatically under pressure [59], Gill *et al.* [16] report only a 10 to 20 percent conductivity increase under 10 Kbar.

The optical properties show that a strong red-shift of the plasma edge occurs on bromination (see Figure 6) [9,10,11]. However, Drude-Lorenz analysis indicate little or no change in plasma frequency or optical scattering time. The shifted plasma edge, which accounts for the observed color change, is accounted for by an increased background dielectric constant on bromination.

The effects of bromine incorporation on the superconducting properties are particularly interesting since the transition temperature  $T_c$  changes very little [9], while the width of the transition, the pressure dependence of  $T_c$  [99], the Meissner effect [63] and the critical field are strongly affected [105]. Initial measurements of  $T_c$  on  $(\text{SNBr}_{0.4})_x$  crystals showed negligible change from  $(\text{SN})_x$  values [9]. More recent results show an increase of about 20 percent in  $T_c$  on bromination [100]. The transition is much sharper in  $(\text{SNBr}_{0.4})_x$  than in  $(\text{SN})_x$  as can be seen in Figure 7. The broad transition in  $(\text{SN})_x$  has been partly ascribed to disorder [51]; however, since  $(\text{SNBr}_{0.4})_x$  has considerably more disorder and a sharper transition, the role of the disorder appears not to be dominant in either material. The width of the transition in  $(\text{SN})_x$  is more probably due to superconducting fluctuations, whose absence in  $(\text{SNBr}_{0.4})_x$  is evidence for increased three-dimensionality in this material. The pressure dependence of  $T_c$  is also qualitatively different from  $(\text{SN})_x$  (Figure 8), decreasing monotonically to about 150 mK under 10 Kbar. Dee *et al.* [63] have observed a complete Meissner effect in  $(\text{SNBr}_{0.4})_x$  crystals. A much sharper transition than in  $(\text{SN})_x$  was also observed indicative of more tightly coupled fibers. Critical field studies by Kwak *et al.* [100] show that in contrast to  $(\text{SN})_x$ ,  $H_c$  is well-behaved and can be treated by anisotropic three-dimensional Ginzburg-Landau theory. These data are consistent with increased interfiber coupling in  $(\text{SNBr}_{0.4})_x$ .

Magnetic susceptibility measurements on brominated  $(\text{SN})_x$  show a small Curie-like contribution below 30K [95]. An upper limit of  $2 \times 10^{-4}$  molar for the concentration of spin 1/2 species such as  $\text{Br}_2^-$  is obtained for  $(\text{SNBr}_{0.4})_x$ . Above 30K susceptibility increases linearly with temperature [95].

Conductivity and magnetoresistance measurements on  $(SN)_x$  exposed to bromine, iodine and ICl have been reported by Philipp and Seeger [101]. Only bromine significantly improved the conductivity in these experiments. Halogen treatment enhances a negative magnetoresistance component which is attributed to increased  $(SN)_x$  chain interruptions.

#### 4. MODEL FOR $(SNBr_{0.4})_x$

In the preceding two sections we have seen that although dramatic changes in the appearance, structure and electronic properties occur on bromination of  $(SN)_x$ , closer examination shows that the basic features (both structural and electronic) remain those of  $(SN)_x$ . From electron microscopy we see an almost unchanged  $(SN)_x$  diffraction pattern with increased disorder and a superimposed superlattice structure. In the electronic properties we see an unchanged plasma frequency and an almost unchanged superconducting transition temperature. Clearly the model of  $(SNBr_{0.4})_x$  accounting for these observations must retain many of the features of pristine  $(SN)_x$ . In the present section we will outline the model for  $(SNBr_{0.4})_x$  which emerges from the wide range of experimental observations.

From spectroscopic data we know that the bromine intercalate is incorporated as  $Br_2$  and  $Br_3^-$ , and that both species are aligned parallel to the  $(SN)_x$  chain axis. The decrease in  $d(10\bar{2})$  indicates that bromine is not intercalating between  $(10\bar{2})$  planes, but is entering substitutionally to occupy chain sites. Observation of the "2b" superlattice implies periodic ordering of the bromine only in the direction parallel to the  $(SN)_x$  chains. Geometrical considerations suggest that  $Br_3^-$  ions are responsible for the superlattice structure. Because bromine bonds to sulfur more readily than to nitrogen, the bromine

molecular species can be expected to align along the chain axis so as to maximize sulfur-bromine interactions and minimize nitrogen-bromine interaction.

Because of the fibrous morphology of  $(SN)_x$  bromine will also be incorporated between fibers. As the fiber diameter decreases, the amount of bromine attached to fiber surfaces becomes significant relative to the amount intercalated within the fibers. For  $(SNBr_{0.4})_x$  with approximately 30 Å diameter fibers, all the bromine could be accommodated as a monolayer on these fiber surfaces. Thus a structural model emerges of 30 Å diameter  $(SN)_x$  fibers with a monolayer coating of aligned  $Br_3^-/Br_2$  ordered along the b-axis with a repeat of 2b due to preferential sulfur bonding conditions [24]. The remaining  $Br_2$  and  $Br_3^-$  is thought to be incorporated within the fibers accounting for the changed lattice parameters.

How does this model for the structure of brominated  $(SN)_x$  account for the dramatic changes in the electronic properties? The large increase in conductivity and the approximately constant plasma frequency suggest that the main effect of bromination is to increase the dc scattering lifetime [9]. Increased free carrier density due to charge transfer from free bromine cannot itself account for the tenfold increase in conductivity. In  $(SN)_x$  the resistivity has a  $T^2$  dependence suggesting that electron-hole scattering is the dominant lifetime limiting process [58]. The Fermi surface geometry is consistent with an efficient electron-hole scattering mechanism. Gill et al. [9] have suggested that the increased conductivity of brominated  $(SN)_x$  is due to suppression of electron-hole scattering due to Fermi surface changes brought about by bromination. Assuming that charge transfer from bromine removes approximately 0.1 electrons/SN unit from the conduction bands, the Fermi level is lowered by about 1eV. Lowering  $E_F$  strongly affects

the shape of the Fermi surface, expanding the volume of the hole pockets and shrinking or even eliminating the electron pockets. Such changes in the Fermi surface will certainly drastically alter the special conditions favoring efficient Umklapp electron-hole scattering. The assumed charge transfer of 0.1 electron/SN unit is consistent with the small plasma frequency change observed optically. Elimination of electron-hole scattering through acceptor doping with bromine increases the dc-lifetime and therefore the conductivity, since now only the phonon scattering channel limits lifetime. The change from electron-hole to electron-phonon scattering should be manifested in a change from  $T^2$  to a linear temperature dependence for resistivity. In addition, one expects a much reduced pressure dependence of conductivity in brominated  $(SN)_x$  since electron-phonon scattering processes will not be as sensitive to the shape of the Fermi surface. In fact, the pressure dependence of conductivity for brominated crystals is greatly reduced compared to  $(SN)_x$  and can be adequately accounted for by lattice stiffening effects usually dominant in metals. Thus this model invoking the Fermi surface changes due to charge transfer on bromination and subsequent suppression of electron-hole scattering explains the major features of the electronic properties of brominated  $(SN)_x$  [60].

#### IV. POLYACETYLENE

##### A. Chemistry of Polyacetylene

Although polyacetylene,  $(CH)_x$ , has long been of interest to theoreticians as the ultimate member of the polyene family, the experimental study of this material was impeded for some time by its intractable nature. Natta first reported a synthesis of polyacetylene from acetylene using a Ziegler-Natta catalyst over 20 years ago, but the polymer produced was a black, insoluble, air-sensistive powder with neither a melting point nor a glass transition temperature [13]. Despite the materials limitations it was

recognized that this material might exhibit interesting transport properties. Thus, Hatano carried out early electrical measurements which showed that  $(CH)_x$  is a wide band gap semiconductor [102]. Even more interesting were the results of Berets and Smith who showed that the conductivity of compressed pellets of polyacetylene could be systematically varied from  $10^{-9}$  to  $10^{-2} \text{ ohm}^{-1}\text{-cm}^{-1}$  by exposure to various Lewis acids and bases [14]. These results aroused little interest, however, particularly in light of the dubious purity and uncertain structure of the polymer.

A major breakthrough in the synthesis and characterization of  $(CH)_x$  occurred in 1971 when Shirakawa and Ikeda were able to form polyacetylene films by the polymerization of acetylene on the surface of a highly concentrated Ziegler-Natta catalyst solution [103]. These flexible films share the air sensitivity and insolubility of the earlier Natta powders, but the physical continuity and convenience of handling of polyacetylene in this new form provided the impetus for a more detailed investigation of the structure and properties of this interesting material.

Films of polyacetylene exhibit a metallic luster and appear to the eye to be continuous, but microscopic investigation of the morphology of these materials by scanning electron microscopy reveals an open fibrillar structure [15]. The films consist of interwoven fibers approximately  $200\text{\AA}$  in diameter. Although the flotation density of polyacetylene is approximately  $1.2\text{g/cc}$ , the bulk density is only  $0.4\text{g/cc}$  [15,104]. Film formation at high catalyst concentrations appears to involve a physical meshing of these growing fibers. Indeed, at lower concentrations of the same catalyst no film is formed, apparently because the individual powder particles settle from solution before meshing of the fibers can occur. By combined mechanical and thermal treatment Shirakawa has been

able to obtain partial alignment of the fibers in a polyacetylene film [105]. As expected such stretch aligned films exhibit anisotropic electrical and optical properties [106,107].

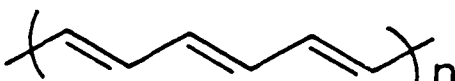
Shirakawa and co-workers examined a number of Ziegler-Natta catalysts, obtaining optimum results with a 4:1 mixture of triethylaluminum and titanium tetra-n-butoxide [15]. Subsequent investigations on polyacetylene have primarily employed material made using this catalyst formulation with a few notable exceptions. Wnek *et al.* have used a modification of the Shirakawa conditions to obtain polyacetylene as a foam, whose electrical properties are similar to those of polyacetylene film, but whose physical form presents interesting possibilities for potential applications [108]. Wegner's group has made extensive use of the Luttinger catalyst, a mixture of  $\text{Co}(\text{NO}_3)_2$  and  $\text{NaBH}_4$  [109]. This latter procedure also produces polyacetylene in the form of films, and as discussed below Wegner has used results obtained with these materials to challenge the accepted models for both the structure and mechanism of charge transport in polyacetylene. However, the question of whether the Shirakawa and Luttinger polymers exhibit identical morphologies remains open. Finally the synthetic approach of Edwards and Feast deserves mention [110]; using a polymeric precursor, these authors have attempted to introduce the conjugated double bonds of polyacetylene via a thermal extrusion reaction. Although the material produced was similar to polyacetylene spectroscopically, the decomposition of the starting polymer was apparently incomplete. Nevertheless, this general approach is probably worthy of continued examination.

Considering both geometric and rotational isomers, there are four possible planar structures (I-IV) for the polyacetylene backbone. Based on infrared and Raman assignments and comparisons with model compounds, Shirakawa has found that

Ziegler-Natta polymerization at  $-78^{\circ}\text{C}$  produces exclusively the *cis-transoid* structure (I) [15]. Polymerization at  $150^{\circ}\text{C}$ , on the other hand, yields only the *trans-transoid* product (II). Syntheses carried out at intermediate temperatures provide mixtures of I and II. The *cis-transoid* structure may also



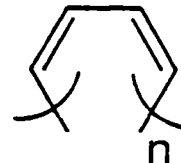
I



II



III



IV

be converted to *trans-transoid* by heating at  $200^{\circ}\text{C}$  for one hour [111]. Although the *trans-cisoid* structure (III) may be an intermediate in this thermal isomerization, there is no evidence for its independent existence. Structure IV, the *cis-cisoid* isomer, is also not observed (and in fact cannot be rigorously planar for more than two repeat units). Adopting the common usage we will refer below to structures I and II as *cis* and *trans*, respectively.

Based on X-ray measurements Shirakawa has estimated polyacetylene produced with the Ziegler-Natta catalyst to be approximately 85% crystalline but highly disordered [112]. This disorder leads to broadening of the X-ray diffraction peaks and generally makes it quite difficult to determine the crystal structure of either polyacetylene isomer.

Using a combination of the observable diffraction peaks, molecular packing considerations, and model compound geometries, Baughman has proposed structures for both *cis*- and *trans*-polyacetylene [104,113,114]. Significantly, the chain axes in both structures are predicted to lie along the fiber axis. This orientation was also suggested by early electron diffraction measurements [115]. Recently, however, Wegner has interpreted a more complete analysis of electron diffraction data in terms of a chain-folded structure similar to that observed in polyethylene and other organic polymers [116]. On the other hand, Chien and Karasz have also carried out an extensive analysis of electron diffraction data which they believe supports the Baughman model [117]. Obviously the resolution of this problem is critically important to the interpretation of the wide variety of physical measurements which have been carried out on polyacetylene.

An equally important unresolved question involves the extent of crosslinking in polyacetylene. In an early  $^{13}\text{C}$  NMR experiment Waugh observed approximately 5%  $\text{sp}^3$  carbons, which he suggested might represent crosslinking sites [118]. However, subsequent NMR experiments have been unable to detect any  $\text{sp}^3$  carbons, placing an upper limit (essentially the experimental limits of detection) of 1% on the extent of crosslinking [119]. Of course, one crosslinking site for every 100 carbons would still represent an extensive perturbation of the polyacetylene structure. More recently, Wegner has suggested that although the  $(\text{CH})_x$  produced by Ziegler-Natta catalysis is highly crosslinked, polyacetylene synthesized using the Luttinger catalyst is virtually free of crosslinks [109]. No in depth investigation of the differences in spectroscopic and transport properties of these two forms of polyacetylene has yet been carried out.

This detailed examination of the structure and properties of polyacetylene was, of course, prompted by the finding that the conductivity of polyacetylene could be raised to quite high levels by exposure to oxidizing or reducing agents [120]. Whereas *cis*- and *trans*-polyacetylene have conductivities of  $\sim 10^{-9}$  ohm $^{-1}\text{-cm}^{-1}$  and  $10^{-5}$  ohm $^{-1}\text{-cm}^{-1}$ , respectively, treatment of these films with, for example, AsF<sub>5</sub> leads to conductivities as high as 1000-2000 ohm $^{-1}\text{-cm}^{-1}$ . (For better or worse, in analogy with more traditional semiconductor terminology this process has generally been referred to as "doping".) Lightly doped samples exhibit intermediate conductivities. At room temperature the conductivity of heavily doped samples shows a metallic temperature dependence, but at lower temperatures the conductivity is activated [121]. Oxidized polyacetylene is a p-type conductor while reduced polyacetylene is n-type [122,123]. Oxidation of stretch-aligned films (draw ratio of three) results in a conductivity of approximately 3000 ohm $^{-1}\text{-cm}^{-1}$  along the direction of orientation while the conductivity perpendicular to the stretching axis is a factor of 16 lower [106].

After considerable initial debate as to the actual mechanisms of the doping reactions, it is now generally accepted that all dopants can be divided into three general groups. The first type consists of oxidizing agents like arsenic pentafluoride, iodine, bromine, and certain transition metal salts. These dopants function by removing electrons from the polymer  $\pi$  system to produce a delocalized cation or polycation [124]. In contrast, the second group of dopants is composed of reducing agents, such as sodium metal or sodium naphthalide, which act by donating electrons to the polymer  $\pi$  orbitals to generate delocalized anionic species. Oxidation and reduction may also be achieved electrochemically [125,126]. X-ray diffraction studies on the oxidized polymer indicate

that the dopant moieties physically intercalate between the  $(CH)_x$  chains in heavily doped samples [127,128].

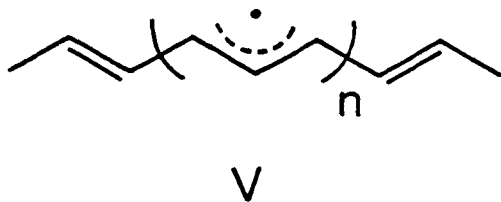
The third type of polyacetylene doping involves strong proton acids. Gau et al. initially showed that exposure of  $(CH)_x$  films to the vapors over perchloric or sulfuric acid led to conductivities as high as  $1000 \text{ ohm}^{-1}\text{-cm}^{-1}$  [129]. There was, however, some question as to whether the acids themselves were the true dopant species, since the anhydrides of both of these acids are quite strong oxidants and would be expected to be effective oxidants of polyacetylene in their own right if present in trace amounts in these experiments. This question became even more significant when it was shown that hydrogen bromide and hydrogen chloride, acids without oxidizing anhydrides, are at best weak dopants of  $(CH)_x$  in the gas phase. The reality of proton acid doping was eventually demonstrated using trifluoromethanesulfonic acid, whose anhydride can be shown not to dope  $(CH)_x$  [130], and anhydrous hydrogen fluoride [131]. Each of these species proves capable of doping polyacetylene to metallic levels.

The precise mechanism of proton doping remains undetermined, but logical speculation suggests that the reaction proceeds by addition of a proton to a double bond. This new  $sp^3$  position then splits the chain into two segments, one a shorter length of neutral polyacetylene and the other a delocalized cation like that produced in normal oxidative doping. Using compensation experiments McQuillan has detected the presence of  $sp^3$  infrared absorptions in HF doped samples [131]. These  $sp^3$  sites would appear to create a serious disruption of the original extended  $\pi$  conjugation of polyacetylene, particularly at the high doping levels used to obtain metallic conductivities. Just how such a system could support effective electrical transport remains unclear.

One shortcoming of the above doping techniques is that they do not allow specific reaction of only selected areas of a given polyacetylene film. Because of the highly porous nature of  $(CH)_x$ , gas phase or solution doping using a conventional masking technique cannot be used to generate conducting or semiconducting patterns in a film. Attempts at using ion implantation to dope polyacetylene have provided mixed results. Recently, Clarke *et al.* have provided an alternate approach to this problem using diaryliodonium or triarylsulfonium salts [132]. These materials are inert toward polyacetylene under normal conditions and may be impregnated into  $(CH)_x$  films without affecting their conductivity. On ultraviolet irradiation, however, these salts decompose to yield strong proton acids which, as noted above, are effective dopants of polyacetylene. In this case simple radiation masks allow selective doping of only those areas of a film exposed to UV light. This technique also allows one to achieve a desired doping level quite conveniently by controlling the amount of salt impregnated into the polymer.

Although the chemistry involved in these various doping processes is now fairly well understood, the means by which these reactions promote high electrical conductivity in polyacetylene is a source of some controversy. Originally the conductivity enhancement was interpreted in terms of straightforward removal of electrons from the valence band (oxidative doping) or addition of electrons to the conduction band (reductive doping) in analogy to the established mechanisms for the doping of traditional semiconductors. More recently, however, an alternate explanation invoking a novel soliton theory has been advanced to explain the doping of polyacetylene. Stimulated by the general current interest in solitons [133] in both the theoretical and solid state physics communities, this theory has received considerable attention and some experimental support.

The soliton theory actually attempts to explain two superficially unrelated features of polyacetylene: the nature of the large number of free spins in undoped *trans*-(CH)<sub>x</sub> and the mechanism by which electrical conductivity is enhanced on oxidation or reduction of the polymer. Ironically this theory was first postulated in somewhat simpler form in 1962 in an insightful paper by Pople and Walmsley [134] on possible defect states in extended polyenes, but was rather quickly rejected by experimentalists. Essentially Pople and Walmsley suggested that delocalized species like Structure V might contribute significantly to the high number



of free spins observed in conjugated polymers (one spin for every 3000 carbons in *trans*-polyacetylene). However, the prediction that these defects should be thermally populated ( $E_a \sim 0.2\text{eV}$ ) was quickly refuted experimentally [135].

Pople's suggestion was revived in 1979 independently by Rice [136] and by Su, Schrieffer and Heeger [137], who realized that this defect site could be described as a soliton domain wall separating two energetically equivalent but topologically distinct segments of *trans*-polyacetylene. Although these defects were again predicted to be accessible thermally, a somewhat higher  $E_a$  was calculated ( $\sim 0.4\text{eV}$ ) and the observed spins were suggested to be defects generated irreversibly during the *cis-trans* isomerization. These domain wall defects, often called neutral solitons, are predicted to be highly mobile along the *trans*-polyacetylene chain. It is important to understand that

such mobile defects are impossible in *cis*-polyacetylene, where an equivalent defect would separate the chain into energetically inequivalent *cis-transoid* and *trans-cisoid* structures, leading to pinning of the defect at a chain end. (In fact few or no free spins are observed in pure *cis*-polyacetylene [138], but this is only an indication of a low defect level and not a consequence of any soliton-like behavior.)

The neutral soliton model predicts that the mobile spins in *trans*-polyacetylene should show motionally-narrowed EPR signals with little or no resolved hyperfine coupling. Experimentally these features are, indeed, observed [139,140]. Moreover, Nechtschein has used dynamic nuclear polarization (DNP) experiments and proton T<sub>1</sub> measurements to show not only that the spins in *trans*-polyacetylene are moving very rapidly ( $\sim 10^{13}$  rad/sec), but that their motion is extremely one-dimensional, with a ratio of the diffusion rates along and transverse to the chains greater than 10<sup>6</sup> [141]. Although the absolute magnitude of the spin diffusion rate along the chain has been questioned [142], the observation of an Overhauser effect in the DNP experiments certainly places a lower limit of  $\sim 5 \times 10^{10}$  rad/sec on the diffusion rate [141]. These results provide the strongest experimental support for the presence of neutral solitons in undoped polyacetylene, although Etemad has recently suggested that the soliton theory may also be necessary to explain phototransport effects in *trans*-polyacetylene [143,144].

The more controversial aspect of the soliton theory involves the actual mechanism of polyacetylene doping. According to this theory initial reaction takes place at neutral soliton sites to provide charged defects (VIa for oxidation, VIb for reduction) which also



may be described as soliton domain walls [136,137]. However, the relatively low number of neutral solitons allows this mechanism to account only for the first ~0.03% of doping. The important prediction of the soliton mechanism is that subsequent doping also serves to generate charged solitons from defect free regions of the polyacetylene chain. Energetically this is favorable because it only costs 0.4eV to create a soliton (neutral and charged solitons are of equal energy), while removal of an electron from the valence band or addition of an electron to the conduction band costs 0.7eV, one-half the band gap [137]. These charged solitons initially form states at the band center which are localized by the coulombic attraction of the dopant counterion. Ultimately screening occurs and the solitons form a band at the gap center. This stage would correspond to the semiconductor-to-metal transition observed at approximately 1% doping. Continued doping would cause broadening of the soliton band and eventual overlap with the valence and conduction bands. Because the charged solitons are spinless, a unique prediction of the soliton mechanism is that doped polyacetylene should show metallic behavior above the semiconductor-to-metal transition, but that there should be no Pauli susceptibility observed until overlap of the soliton band with the valence and/or conduction bands occurs [145]. At this point the system can be described by a typical single particle band picture and the usual properties of a metal, including Pauli susceptibility, should be found.

The extent of experimental support for the soliton doping mechanism has been the source of considerable controversy. Ikehata *et al.* have observed that, under very carefully controlled conditions,  $\text{AsF}_5$  doping leads to a loss of essentially all Curie spins by 1% doping accompanied by very low levels of Pauli susceptibility until approximately 7% doping, at which point a rather dramatic increase in Pauli susceptibility is observed [145]. These results are, of course, quite consistent with the predictions of the soliton model. On the other hand, in their attempts to repeat the Ikehata experiments, Tomkiewicz *et al.* observed a continuously increasing Pauli susceptibility as a function of dopant concentration, even in samples below the 1% doping level [146]. These results were interpreted in terms of inhomogeneous doping, where, for one reason or another, metallic "islands" are formed at very low doping levels and grow in size and/or number as doping progresses [147]. The semiconductor-to-metal transition is then better understood as a percolation threshold. AC conductivity measurements [148] and the non-ohmic behavior of the samples in electric fields [149] support this picture of inhomogeneity in the doping process.

Initially it was suspected that the difference between these two apparently contradictory sets of results lay in subtle differences in sample preparation. Joint experiments have revealed, however, that the actual difference involves the measurement techniques employed [150]. Both groups obtain similar results throughout the doping range when using X-band EPR spectroscopy to measure the susceptibility. Above  $\sim 1\%$  doping there is a systematic deviation between results from the Schumacher-Slichter technique (used by Ikehata *et al.* [145] and those from X-band EPR measurements (used by Tomkiewicz *et al.* [146,147]). Since skin depth problems become increasingly severe in the EPR measurements as the doping progresses above 1%, one would expect the

Schumacher-Slichter results to be more reliable in this region. Although a complete resolution of these discrepancies has not yet evolved, several conclusions can be drawn at this point. There is certainly a dramatic transition in the Pauli susceptibility above 7% doping, consistent with the predictions of the soliton mechanism. On the other hand, there is a finite, measureable Pauli susceptibility observable in samples doped to concentrations below 7%. In particular, this is true for samples in the 0.2-1.0% range, below the semiconductor-to-metal transition. This Pauli susceptibility undoubtedly reflects the nonuniformity of the doping process, even under conditions designed to minimize inhomogeneity. The extent to which this nonuniformity plays a role in the transport properties at low doping levels remains unresolved.

In another experimental probe of the magnetic properties of  $(CH)_x$ , Peo *et al.* examined the magic angle  $^{13}\text{C}$  NMR spectrum of polyacetylene as a function of  $\text{AsF}_5$  doping [151]. They saw no indication of a Knight shift of the carbon signal by carrier spins until 7% doping, although conductivity measurements clearly showed a semiconductor-to-metal transition in their samples at a doping level of roughly 1%. Subsequent experiments by Clarke and Scott, however, have revealed the presence of a shifted peak in  $\text{AsF}_5$  doped samples at doping concentrations as low as 1% [152]. They attribute the bulk of the shift to a chemical shift arising from the removal of electrons from the polymer  $\pi$ -system in the doping process, with any Knight shift representing a smaller contribution superimposed on the chemical shift. These latter results also demonstrated for the first time a difference in the degree of homogeneity of doping between *cis* and *trans* polyacetylene. Although *trans* samples appear somewhat inhomogeneous, the *cis* samples at, e.g., 3% doping appear to consist of heavily doped

regions and essentially undoped regions. This observation suggests that comparisons between lightly doped *cis* and *trans* samples should be made very cautiously.

Infrared spectroscopy has also provided a measure of support for the soliton doping mechanism. Rice and Mele have carried out extensive calculations of the infrared features expected in a polyacetylene sample containing nonoverlapping charged solitons [153]. Their predictions are in quite good agreement with the infrared spectrum of lightly doped polyacetylene [154]. Interpretation of the infrared data must, however, take into account the remarkable similarity in the IR spectra of lightly and heavily (10%) doped polyacetylene [154,155], even though the soliton model is not expected to be applicable at high doping levels.

## B. Electronic Properties

### 1. BAND STRUCTURE

Even before the highly conducting properties of doped  $(CH)_x$  films were discovered, there was considerable interest in the band structure of this prototype infinite polyene system [12]. This interest arose from speculation on the physical properties to be expected from infinite polyene chains. The methods of calculation applied to this system have addressed the issue of the adequacy of a single particle band description and the merits of including electron correlation effects. Unfortunately, widely different results have been reported for these calculations. With the discovery of the metallic properties of doped  $(CH)_x$ , band structure calculations have received renewed attention stimulated by the desire to obtain a theoretical basis for understanding the electronic properties of both intrinsic and doped material. A number of band structure calculations appear in the recent literature on both the *trans*- and the *cis*- $(CH)_x$  conformations.

Calculations of the single particle band structures of *cis-transoid* and *trans-(CH)<sub>x</sub>* were made by Grant and Batra [156] using both the LCAO extended tight-binding method and the semiempirical extended Hückel method. For the *cis-transoid* calculations the crystal structure proposed by Baughman *et al.* [114] was used. For *trans-(CH)<sub>x</sub>* different carbon-carbon bond length schemes were used including uniform bonds and both weakly alternating and strongly alternating bond lengths. The *cis-transoid* isomer was found to have a band gap of 1.2eV and conduction and valence band widths of nearly 6eV for directions parallel to the chains. For the *trans-(CH)<sub>x</sub>* the degree of bond alternation has a profound effect on the calculated band gap. For uniform bonds the Fermi level passes through a degeneracy point at the Brillouin zone edge and the system is intrinsically metallic. With increasing bond alternation a single particle band gap exists which increases to 2.3eV for typical single and double lengths.

Band structures for the *trans*, *cis-transoid* and *trans-cisoid* conformations have been calculated by Kasowski *et al.* [157] using an extended muffin tin orbital method. This study shows that *(CH)<sub>x</sub>* is an intrinsic semiconductor with energy gaps of 1.6, 1.7 and 1.2eV, respectively, for the *trans*, *cis-transoid* and *trans-cisoid* structures. Three-dimensional charge density contour plots show that the bonding orbitals are C- $\pi$ -like, sticking out from the plane of the molecule. These  $\pi$ -states, which are responsible for the semiconducting gap, are also expected to react with dopants.

Yamabe *et al.* [158] have compared the calculated band structure properties of the *cis-transoid* and the *trans-cisoid* structures of *(CH)<sub>x</sub>*. From total energy/unit cell,  $\pi$ -bond order and interatomic interaction energy comparisons these authors conclude that the *cis-transoid* isomer is the favored *cis*-structure of *(CH)<sub>x</sub>*.

The band calculations on heavily doped *trans*-(CH)<sub>x</sub> by Kasowski *et al.* [159] are of considerable interest. Extended muffin-tin orbital calculations were made on defect-free material and material heavily doped with AsF<sub>5</sub>, AsF<sub>6</sub><sup>-</sup>, SbF<sub>6</sub><sup>-</sup> and PF<sub>6</sub><sup>-</sup>. For the hexafluoride dopants, AsF<sub>6</sub><sup>-</sup> and SbF<sub>6</sub><sup>-</sup>, hybridization of metal s-states with polymer  $\pi$ -states produces a partially filled metallic band implying strong metallic conductivity along chains and weaker metallic conductivity between chains. Doping with AsF<sub>5</sub> yields a semiconductor with a completely filled As s-valence band and an empty  $\pi$ -conduction band. Doping with PF<sub>6</sub><sup>-</sup> yields an empty P s-band, but charge transfer to F atoms partly empties a  $\pi$ -band implying metallic conductivity along, but not between, chains. The results for AsF<sub>5</sub> and AsF<sub>6</sub><sup>-</sup> doping are particularly important since they give theoretical support for AsF<sub>6</sub><sup>-</sup> as the effective dopant in highly conducting *trans*-(CH)<sub>x</sub>. On the other hand, many dopants which would not be expected to undergo this sort of hybridization are also effective dopants of polyacetylene.

## 2. SEMICONDUCTOR PROPERTIES

Unlike the polymeric metals we have described so far in this chapter, undoped (CH)<sub>x</sub> is an intrinsic semiconductor. Although it was the metallic properties of the heavily-doped material which stimulated recent interest, the semiconducting properties of intrinsic and lightly-doped (CH)<sub>x</sub> are of considerable interest. In particular the mechanism of doping and the proposed soliton transport models are areas of great importance and considerable controversy. Junction studies in which (CH)<sub>x</sub> is the active semiconducting element also place strong emphasis on the properties of intrinsic and lightly-doped material.

Band structure calculations described in the previous section indicate that both *cis* and *trans* isomers of  $(CH)_x$  should be relatively wide band semiconductors with band gaps in the range of 1.2 to 1.7 eV. Photovoltaic threshold measurements by Tani *et al.* [160] on In/ $(CH)_x$  Schottky barriers have yielded a value of 1.49 eV for the single particle band gap of the *trans*-isomer. Optical absorption [107], photoconductivity [160] and photoelectrochemical cell studies [161] also indicate a band gap of this magnitude.

Electrical conductivity measurements on  $(CH)_x$  films doped with halogens and arsenic pentafluoride,  $AsF_5$ , were first reported by Chiang *et al.* [16]. The room temperature conductivity of the undoped *trans*-isomer is about  $2 \times 10^{-5} \text{ ohm}^{-1}\text{cm}^{-1}$ . For the *cis*-isomer, the room temperature conductivity is considerably lower with a value of about  $2 \times 10^{-9} \text{ ohm}^{-1}\text{cm}^{-1}$ . The conductivity of both isomers increases on exposure to a wide range of dopants. However, doping of the *cis*-isomer results in isomerization to the thermodynamically stable *trans* form [15,111] so that lightly-doped initially *cis* films become heterogeneous systems. With heavier doping, induced isomerization can be detected by optical absorption, thermopower and NMR second moment techniques.

Plots of  $\ln\sigma$  versus  $1/T$  for undoped and lightly-doped *trans*-( $CH)_x$  show activated-like behavior but with some curvature, which probably indicates a distribution of activation energies [162]. For undoped *trans*-( $CH)_x$  the slope at room temperature yields an activation energy of 0.3 eV. This activation energy is relatively insensitive to dopant concentration up to about 0.1 mole % and then decreases rapidly as the material undergoes a semiconductor/metal transition at dopant concentrations near 1 mole %.

Thermoelectric power (TEP) measurements by Park *et al.* [162,163] and by Kwak *et al.* [121,164] are in good agreement for the entire dopant concentration range from undoped semiconductor to heavily-doped metallic behavior. For the undoped *trans*-isomer a value of about +90 uV/K is obtained. For acceptor dopant concentrations below 0.1 mole % there is little change in thermopower. As the dopant concentration is increased from 0.1 mole % to 1 mole % the thermopower decreases drastically to a value characteristic of the metallic state (about 10 uV/K). The relative insensitivity of TEP to concentration below  $10^{-1}$  mole % has been cited as evidence for a defect or impurity concentration of about 0.1 mole % in pristine  $(CH)_x$ . At low dopant concentrations, Park *et al.* [162] find that TEP is essentially temperature independent which is interpreted in terms of a dilute concentration of carriers hopping in a set of localized states. From the temperature independence of TEP, implying a constant carrier density of about  $2 \times 10^{18} \text{ cm}^{-3}$  for undoped *trans*-( $CH)_x$ , and from the activated conductivity, Park *et al.* [162] conclude that the mobility is activated in the dilute limit with a magnitude of about  $5 \times 10^{-5} \text{ cm}^2/\text{V}\cdot\text{sec}$  at room temperature. Since in the metallic regime the mobility is estimated to be about  $60 \text{ cm}^2/\text{V}\cdot\text{sec}$ , an abrupt change of 5 to 6 orders of magnitude in carrier mobility is assumed to occur on passing through the semiconductor/metal transition at dopant concentrations near 1 mole %. The low mobility of the undoped  $(CH)_x$  is unexpected for a wide band semiconductor. The inference that transport is by a localized state hopping mechanism is argued to be qualitatively consistent with the proposed soliton doping mechanism discussed in more detail above.

Measurements of the electric field, E, dependence of conductivity of lightly  $\text{AsF}_5$  doped *cis*-( $CH)_x$  have been reported recently by Mortensen *et al.* [151]. In the high field

regime (at T=4K) the resistance  $R_H$  was of the form

$$R_H = R_{H_0} \exp(E_0/E).$$

In the low-field regime the temperature dependence of resistance  $R_L$  fits the relationship

$$R_L = R_{L_0} \exp(T_0/T)^{1/2}.$$

These field and temperature dependences are compared with the expected behavior of granular metals in a concentration regime in which isolated metallic particles are dispersed in a dielectric continuum.

### 3. METALLIC PROPERTIES

The metallic properties of heavily-doped  $(CH)_x$  films have been more extensively investigated at this time than the semiconducting properties. This emphasis on the highly conducting state was a consequence of interest in the highly conducting polymers and the quasi one-dimensional organic charge transfer salts. This interest was further sharpened when doped  $(CH)_x$  was shown to have the highest conductivity of any organic material excluding intercalated graphite. Considering the matted fibrous structure of  $(CH)_x$  films and the highly reactive nature of the dopants involved, it is remarkable how reproducible transport results have been for experiments in a number of laboratories. The earliest indications of high conductivity in heavily doped  $(CH)_x$  were obtained in the experiments of Berets and Smith [14] in which  $(CH)_x$  powder was exposed to strong oxidants including the halogens. The pellet conductivity was observed to increase by several orders of magnitude. However, the discovery by Ito, Shirakawa and Ikeda [15] of a process for forming continuous films of  $(CH)_x$  was the key to subsequent research on the electronic properties of this polymer. In 1977 Chiang *et al.* [16] reported doping experiments on

(CH)<sub>x</sub> films showing a metal/insulator transition for an acceptor dopant concentration near 1 mole % and a maximum conductivity comparable to that of single crystals of the organic metal TTF-TCNQ. Subsequent experiments demonstrated high conductivity by exposure to donor dopants (alkali metals) [123] and conductivities as high as  $3000 \Omega^{-1}cm^{-1}$  by using stretch oriented (CH)<sub>x</sub> films [106].

In spite of the magnitude of the conductivity of heavily doped films, which clearly indicates metallic behavior, the temperature dependence is not characteristic of a metal. Figure 9 shows the temperature dependence of conductivity for highly doped and intermediate doped *trans*-(CH)<sub>x</sub> films. In heavily doped material, the conductivity increases slightly with decreasing temperature for  $T \geq 220K$  [122]. As the temperature is decreased further to 4K, the conductivity decreases. However, for temperatures below 4K the conductivity remains constant [121,164]. For more lightly doped samples the conductivity is activated over the entire temperature range.

Thermoelectric power measurements on the highly conducting (CH)<sub>x</sub> films are of particular interest because they provide a method for evaluating metallic behavior without current flow across barriers associated with the disordered fibrous structure. Kwak *et al.* measured TEP as a function of temperature in  $AsF_5$  doped films [121,164]. For greater than 1 mole % the thermopower was found to be small ( $\approx 10\mu V$  at 300K), positive and independent of concentration. The temperature dependence was linear and extrapolated through the origin as expected for an ideal simple metal. The sign of the thermopower is consistent with the acceptor character of the dopant, and the magnitude and temperature dependence is indicative of intrinsic metallic behavior.

The Hall effect in heavily doped  $(CH)_x$  films has been measured by Seeger *et al.* [122]. The Hall voltage was found to be very small necessitating double phase-sensitive techniques to obtain an adequate signal-to-noise ratio. Measurements were made over the temperature range from 4K to 300K and for acceptor concentrations ( $AsF_5$ ) from 2 mole % to 17 mole %. The sign of the Hall coefficient  $R_H$  is positive and relatively insensitive to temperature ( $R_H$  increases by a factor of 2 or 3 on cooling to 4K). The magnitude of  $R_H$  is very small, which, if interpreted by a simple single band model, yields a carrier concentration two orders of magnitude greater than the dopant concentration. Since in the single band case  $R_H = 1/ne(\mu_H/\mu)$  where  $\mu_H$  is the Hall mobility and  $\mu$  is the conductivity mobility, the data imply that  $\mu_H \approx 10^{-2}\mu$  if the carrier density is assumed equal to the  $AsF_5$  dopant density.

#### 4. JUNCTION PROPERTIES

The intrinsic semiconductor nature of  $(CH)_x$  together with the ability to dope the material with either donor or acceptor molecules forming n- or p-type material has generated interest in junction properties and their possible device applications. The first reports on junction properties of  $(CH)_x$  described rectification properties observed at a crude junction formed by mechanically pressing together sheets of n- and p-type  $(CH)_x$  [81]. Subsequently a number of studies have been reported involving Schottky barriers using heavily doped  $(CH)_x$  as the metal in contact with inorganic semiconductors [165], Schottky barriers in which the  $(CH)_x$  is the semiconductor [160,165], heterojunctions with inorganic semiconductors [165] and electrochemical cells [161] using  $(CH)_x$  as the active photoelectrode.

Schottky barriers were formed by polymerizing  $(CH)_x$  directly on n-type semiconductors (Si and GaAs) and subsequently heavily doping the  $(CH)_x$  with  $AsF_5$  to make it metallic [165]. These junctions had barrier heights in the range from 0.7 to 1.0 volts as estimated from I-V and C-V characteristics. Junction formation showing the p-type conductivity of undoped *trans*-( $CH)_x$  was achieved with pressed contacts of low electronegativity metals (Na, Ba, In) [165].

Extensive studies of Schottky barrier characteristics with undoped and lightly-doped  $(CH)_x$  as the active semiconductor have been reported by Tani *et al.* [160]. Initial experiments were directed toward reliable determination of the band gap of *trans*-( $CH)_x$  by measurement of the photovoltaic effect threshold. With In ( $\phi_M=4.12eV$ ) as the low work function junction metal and Au ( $\phi_M=5.1eV$ ) as the ohmic contact, cells with excellent Schottky barrier I-V and C-V characteristics were obtained. From the photovoltaic response threshold a value of  $1.48eV$  was obtained for the single particle band gap in *trans*-( $CH)_x$ . The band gap was also shown to be independent of doping level for a conductivity range from  $2.6 \times 10^{-4}$  to  $4 \Omega^{-1}cm^{-1}$ .

The junction characteristics of a series of In/ $(CH)_x$  Schottky barriers with a range of doping concentrations have been used to determine mobility as a function of conductivity for  $AsF_5$ -doped *trans*-( $CH)_x$  [166]. From the linear slopes of  $1/C^2$  versus V, characteristic values of the ionized acceptor density  $N_A$  were obtained for each  $(CH)_x$  conductivity. Assuming that the carrier density equals  $N_A$ , mobility values ranging from  $3 \times 10^{-6} cm^2/V\cdot sec$  for undoped  $(CH)_x$  to  $3 \times 10^{-4} cm^2/V\cdot sec$  for lightly-doped ( $\sigma=1 \times 10^{-4} \Omega^{-1}cm^{-1}$ ) material were obtained. These values are consistent with mobilities inferred from doping concentrations by Park *et al.* [162].

Heterojunction formation using p-type undoped *trans*-(CH)<sub>x</sub> in contact with n-ZnS has been demonstrated by Ozaki *et al.* [165]. An open circuit photovoltage of 0.8 volts was observed with significant photosensitivity in the energy range from 1 to 3eV attributed to carrier photogeneration in the (CH)<sub>x</sub>. Another potential solar cell device in which (CH)<sub>x</sub> is the active photoelectrode in an electrochemical cell has been described by Chen *et al.* [161]. This cell consists of undoped (CH)<sub>x</sub> and Pt as electrodes in a sodium polysulfide electrolyte. An open circuit photovoltage of 0.3 volts was obtained with approximately one sun illumination on the (CH)<sub>x</sub>; however, cell efficiency was limited by series resistance and the small effective area of the (CH)<sub>x</sub> electrode.

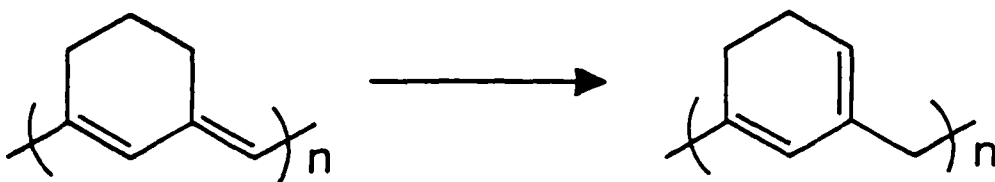
## V. OTHER CONDUCTING POLYMERS

Initially it was hoped that substitution of the hydrogens of polyacetylene with various functional groups would allow the construction of an entire family of conducting polymers whose properties could be controlled in a systematic way. As in the case of (SN)<sub>x</sub> these expectations have not been completely fulfilled, although some progress has been made. Straightforward derivatives of (CH)<sub>x</sub> where alternate hydrogens have been replaced by methyl [167] or phenyl [168] groups, for example, can be synthesized as black powders, but can not be doped to high levels of conductivity with either oxidizing or reducing agents. The failure of these substituted materials to dope to high levels of conductivity is not yet understood. Space filling molecular models suggest that even in the less crowded *trans* form of polyacetylene, substituents which are sterically more demanding than hydrogen (or perhaps fluorine) encounter serious van der Waals repulsions if the polymer backbone is forced to remain planar. Twisting of the backbone relieves the steric interaction, but also diminishes the overlap of the  $\pi$  orbitals along the chain, an effect which would certainly change the electronic properties of the polymer.

On the other hand, these polyacetylene derivatives probably also differ from  $(CH)_x$  itself in terms of molecular weight, morphology, crystallinity, and other parameters whose effects on the doping process are not currently known.

One attractive approach to lessening the steric interaction in polyacetylene derivatives involves the copolymerization of acetylene itself with a substituted acetylene. Chien and co-workers [169] have shown that acetylene and methylacetylene can be copolymerized with the proper choice of catalyst to produce films which can be doped with  $AsF_5$  to conductivities as high as  $50\ \Omega^{-1}\cdot cm^{-1}$ . Varying the ratio of acetylene to methylacetylene in the polymer produces interesting changes in both the electronic and mechanical properties of these films. Thus the ultimate conductivity achieved on  $AsF_5$  doping seems to decrease as the fraction of methylacetylene in the copolymer increases. On the other hand, for compositions containing greater than 50% methylacetylene films are produced which show elastic properties under certain conditions. When dry these films are relatively brittle, but on wetting with solvent they can be stretched quite easily and retain this elongation if dried under tension. Rewetting of one of these stretched films then causes it to revert to its original shape. Unfortunately the copolymers synthesized to date appear to be even more sensitive to oxygen than  $(CH)_x$ .

A more highly substituted derivative of polyacetylene has also been reported. Gibson *et al.* [170] have polymerized 1,6-heptadiyne under homogeneous Ziegler-Natta conditions to produce free standing films with a green-gold metallic luster. Spectroscopic measurements indicate that poly(1,6-heptadiyne) has a conjugated backbone with 6-membered rings fused 1,3 along the chain (VIIa).



Unlike polyacetylene this material is normally amorphous and continuous rather than fibrillar. On doping with iodine the conductivity rises from  $10^{-12} \text{ ohm}^{-1}\text{-cm}^{-1}$  for the pristine polymer to approximately  $10^{-1} \text{ ohm}^{-1}\text{-cm}^{-1}$  for a material of composition  $(C_7H_8I_{1.0})_n$ ; treatment with  $AsF_5$  leads to a maximum conductivity of  $10^{-2} \text{ ohm}^{-1}\text{-cm}^{-1}$ . [171]. The ultimate limitation on the conductivities achieved on doping appears to lie not in the intrinsic electronic properties of the polymer, but rather in the facile rearrangement of the conjugated backbone structure VIIa to the cyclohexadiene structure VIIb, a process which interrupts the conjugation along the polymer chain. This rearrangement is apparently catalyzed by the same species which dope the polymer. Thus the reaction with, for example,  $AsF_5$  actually consists of two competing reactions, a faster oxidation which raises the conductivity of the polymer and a slower rearrangement which reduces the conductivity. This problem eventually limits the applicability of poly(1,6-heptadiyne), but the simple demonstration that this  $(CH)_x$  derivative can be doped to reasonably high conductivities should encourage the search for other conducting derivatives.

MacDiarmid and his co-workers have taken a somewhat different approach to the synthesis of  $(CH)_x$  derivatives [172]. Rather than polymerizing substituted acetylenes, they have produced new materials by carrying out reactions on polyacetylene itself. In particular they have shown that on heating, bromine-doped  $(CH)_x$  evolves HBr and  $Br_2$  to give golden semiconducting films of composition  $(CH_qBr_y)_x$  where  $(q+y)=0.82-0.98$ . Thus a sample of composition  $(CH_{0.82}Br_{0.14})_x$  showed a conductivity of

$2.1 \times 10^{-6}$  ohm $^{-1}$ -cm $^{-1}$ . As with (CH) $_x$  itself, subsequent oxidation of these brominated films with AsF $_5$  or iodine then leads to dramatic enhancements in conductivity with ultimate values on the order of 10 ohm $^{-1}$ -cm $^{-1}$  being achieved. The actual structure of the brominated polymer has not been determined, but in addition to formal replacement of hydrogen by bromine some acetylene formation and crosslinking are believed to occur.

One additional polyacetylene derivative has received considerable theoretical attention, although its actual synthesis has not yet been achieved. Band structure calculations suggest that poly(difluoroacetylene), (CF) $_x$ , should be quite similar to (CH) $_x$  electronically, with the exception that all of the (CF) $_x$  bands should be significantly lower in energy than those of (CH) $_x$  [173]. This suggests that (CF) $_x$  might provide a more stable n-type material than does (CH) $_x$  on treatment with reducing agents. Unfortunately the difluoroacetylene monomer is highly unstable and more elaborate synthetic routes will be required for the generation of this interesting polymer.

Rather than pursuing direct modifications of polyacetylene, several research groups have begun examinations of other polymer systems with conjugated backbones. The first successful demonstration of high conductivity in a nonpolyolefinic organic material involved poly(p-phenylene) (PPP).



PPP

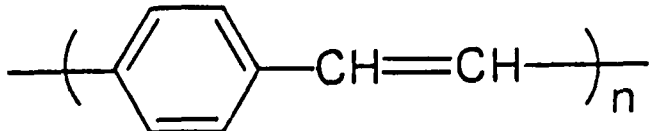
Previous workers had shown that PPP forms charge-transfer complexes with oxidizing agents such as iodine [174], but the conductivities of these complexes never exceeded

$\sim 4 \times 10^{-5}$  ohm $^{-1}$ -cm $^{-1}$ . Using AsF<sub>5</sub>, a considerably stronger oxidant, Ivory *et al.* [175] were able to achieve conductivities as high as 500 ohm $^{-1}$ -cm $^{-1}$ . In comparison the conductivity of undoped PPP is less than 10 $^{-14}$  ohm $^{-1}$ -cm $^{-1}$ . It was also shown that reducing agents such as sodium naphthalide or various alkali metal vapors could be used to generate conducting n-type PPP. The final conductivity of the doped polymer can be varied by controlling the extent and duration of exposure of the PPP to the dopant species. As in the case of polyacetylene, more lightly doped samples behave as semiconductors. Junctions made by pressing together pellets of semiconducting p- and n-type PPP have been shown to exhibit the rectifying characteristics expected for a p-n junction. Hall measurements on heavily AsF<sub>5</sub> doped samples provide an estimate of  $\sim 1$  cm $^2$ /volt-sec for the carrier mobility in these systems. (It is interesting that in PPP reasonable mobilities can be obtained from a straightforward Hall analysis assuming one carrier per dopant molecule, whereas in polyacetylene similar analyses yield physically unrealistic mobilities, presumably because of the complications introduced by the fibrous nature of (CH)<sub>x</sub> films [122].)

In terms of fabricability, poly(p-phenylene) represents less an advance than an alternative to the possibilities offered by polyacetylene, which is essentially limited to films grown on the surface of a Ziegler-Natta catalyst solution as discussed above. PPP as synthesized is an insoluble powder which does not show a glass transition temperature or melting point; however, it is susceptible to high temperature sintering, a powder metallurgical technique which allows the molding of undoped PPP into a variety of shapes. Moreover, Baughman and co-workers have recently developed a unique synthesis of AsF<sub>5</sub> doped PPP which may provide an alternative to this sintering process [176]. Oligomers of poly(p-phenylene), for example biphenyl, terphenyl, and quaterphenyl, form

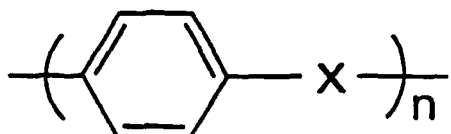
complexes with  $\text{AsF}_5$  which on prolonged exposure to higher pressures of  $\text{AsF}_5$  (~400 torr) are converted to highly conducting materials. Various data suggest that the reaction involved is actually a simultaneous oxidation and polymerization which generates a product quite similar to that obtained by  $\text{AsF}_5$  treatment of PPP. More importantly, when single crystal plates of terphenyl are reacted with  $\text{AsF}_5$  the resulting polymer exhibits strong optical and electrical anisotropy; this type of ordering has not been possible to achieve using PPP itself. Thus the promise of these solid state polymerizations is quite exciting.

Obviously if polyacetylene and poly(p-phenylene) can each be doped to high levels of conductivity, the copolymer consisting of alternating phenylene and double bond units should be an interesting material. Wnek *et al.* have, in fact, examined the properties of this material, poly(p-phenylene vinylene) (PPV) [177].



Pressed pellets of PPV show a conductivity of  $\sim 10^{-10} \text{ ohm}^{-1}\text{-cm}^{-1}$  at room temperature. Exposure to 30 torr of  $\text{AsF}_5$  for 2-3 hours leads to a material of composition  $[\text{C}_8\text{H}_6(\text{AsF}_5)_{0.92}]_x$  which shows a conductivity of  $\sim 3 \text{ ohm}^{-1}\text{-cm}^{-1}$ . The materials examined to date have all been low molecular weight oligomers (degree of polymerization 7-9), primarily due to the insolubility of PPV, which causes its precipitation at early stages of the synthetic reaction. The conductivities observed are quite high for such low molecular weights, however, and may indicate that further polymerization is occurring during the  $\text{AsF}_5$  exposure as in the case of quaterphenyl.

Perhaps the most interesting of the polyphenylene derivatives investigated to date are the heteroatom linked phenylene polymers shown in structure VIII.



In the case where X is oxygen or sulfur these materials are known to exhibit good melt and solution processing characteristics, features which are seriously lacking in the polymers described above. This combination of processibility and the possibility for extended conjugation led two different research groups to independently investigate the doping of these materials [178,179]. Poly(p-phenylene oxide) (X=O) reacts extensively with  $\text{AsF}_5$  but does not produce a material with high conductivity. Treatment of poly(p-phenylene sulfide) (X=S) with  $\text{AsF}_5$ , however, leads to conductivities of  $1\text{-}10 \text{ ohm}^{-1}\text{-cm}^{-1}$  in the resulting polymer.

Poly(p-phenylene sulfide) is a commercially available material [180], which exhibits excellent thermal and chemical stability in addition to the processibility which allows its generation in the form of film, fiber, and monofilament. One must take advantage of these properties before doping, however, since the reaction with  $\text{AsF}_5$  also causes the loss of many of the desirable properties of PPS. The polymer becomes increasingly brittle as the level of doping is raised. The ready processibility of the pristine PPS disappears on doping, as the resulting material shows no melting point or evidence of solubility. The conductivity of the doped polymer is sensitive to heat and exposure to the atmosphere; either treatment leads to an irreversible decrease in the sample conductivity. Despite

these liabilities PPS represents a significant step toward more tractable conducting polymers.

The doping of PPS has also raised several interesting scientific questions. Perhaps the most important arises from an examination of the crystal structure of PPS as determined by Tabor *et al.* [181]. Successive phenylene groups along a polymer chain are twisted at angles of  $\pm 45^\circ$ , a situation which at first seems unlikely to lead to the extended conjugation necessary for conductivity. In their efforts to understand this situation, both the groups at IBM [178] and at Allied [179] have come to the conclusion that on doping PPS is undergoing extensive chemistry in addition to the simple electron transfer proposed for polyacetylene doping [115,124]. The evidence suggests that coupling of phenyl rings is occurring to give either cyclized or crosslinked structures, depending on whether the reacting phenyl groups are on the same or different chains. Indeed, all of the phenylene-type polymers seem to show such extensive chemical modification on treatment with  $\text{AsF}_5$  that the resulting materials remain poorly understood. In this light the mechanisms proposed for the reaction of  $(\text{CH})_x$  with  $\text{AsF}_5$  seem quite remarkable in their relative simplicity.

Heterocyclic aromatic polymers of the general structure IX should also be interesting materials from an electronic point of view. In particular, there exists an extensive literature describing "pyrrole black", a material (or possibly several materials given the general lack of structural characterization) formed by the oxidation of pyrrole under a variety of different reaction conditions. These powders showed generally high conductivities and were often assumed to have structure IX where  $X=N$ .



More recently, Diaz *et al.* [182] have developed a controlled electrochemical synthesis of this polymer, more correctly named polypyrrole, which leads to flexible films with conductivities as high as  $40\text{-}100 \text{ ohm}^{-1}\text{-cm}^{-1}$  [183]. On the basis of electrochemical and spectroscopic data the pyrrole polymerization is believed to involve oxidative coupling at the  $\alpha$ -positions to generate structure IX; simultaneously, however, the polymer is oxidized electrochemically to provide a material of typical composition  $(\text{C}_4\text{H}_{3.4}\text{N}_{0.9})_4(\text{BF}_4^-)$ . The  $\text{BF}_4^-$  is incorporated from the supporting electrolyte as a counterion to the positively charged polymer chain. The polypyrrole is formed on the electrode surface as a smooth continuous film whose thickness can be controlled by monitoring the amount of current passed in the electrochemical cell. Thicker films can be readily peeled from the electrode surface intact. In the absence of air these films can then be repeatedly cycled between the oxidized and neutral (nonconducting) forms by cycling the cell potential. Initial exposure to air leads to a reaction of undetermined nature which causes the polypyrrole to no longer be reducible electrochemically [184]. After the initial reaction with the atmosphere the resulting polypyrrole films still exhibit the same high levels of conductivity. In addition these films are remarkably stable, showing no loss in conductivity after storage in air for several months. Polypyrrole is also considerably more thermally stable than the other doped polymers described above. These unique characteristics should make polypyrrole suitable for a variety of applications without the elaborate protective measures required for other conducting polymers.

A number of N-substituted pyrrole derivatives have also been polymerized electrochemically, but their room temperature conductivities tend to be on the order of  $10^{-3}$  ohm $^{-1}$ -cm $^{-1}$  [185]. Copolymers can also be synthesized readily and show interesting properties. The conductivity of the copolymer of pyrrole and N-methylpyrrole, for example, can be selectively changed from  $10^{-3}$  to  $10^2$  ohm $^{-1}$ -cm $^{-1}$  by varying the mole fraction of N-methylpyrrole in the electrochemical cell from 0 to 1 [184].

Polythiophene (IX where X=S) has been synthesized by both chemical [186,187] and electrochemical [188] techniques. As in the case of polypyrrole, the electrochemically generated polymer is simultaneously oxidized under the reaction conditions. The chemically prepared polymer is subject to subsequent oxidation by iodine. In neither case are high conductivities obtained, however. Typical values are in the range of  $10^{-3}$  to  $10^{-4}$  ohm $^{-1}$ -cm $^{-1}$ . Unlike polypyrrole, the oxidized polythiophene is also unstable in air.

A rather different class of conducting polymers lies outside the scope of this review but deserves mention. Marks and co-workers [189] and Kuznesof *et al.* [190] have used various polymer backbones to hold phthalocyanines in a face-to-face configuration. Partial oxidation of these materials with iodine then provides materials with conductivities as high as 0.1-1 ohm $^{-1}$ -cm $^{-1}$ . However, the conductivity in these polymers is not along the polymer chain itself as in the polymers described above, but is instead similar to that observed in other monomeric stacked phthalocyanine charge-transfer salts.

## VI. CONCLUSION

### A. Potential of Polymeric Metals

Polymers can be made to exhibit semiconducting, metallic, or even superconducting properties not traditionally associated with these materials. This has encouraged the belief that conducting polymers may eventually challenge the more classical materials in certain areas.

It has been suggested that conducting polymers might compete with metals in the area of light-weight wiring. Of the presently known systems only  $\text{AsF}_5$  treated graphite appears to have sufficiently high conductivity [191]. Barrier height measurements of  $(\text{SN})_x$  films and various semiconductor substrates have shown that  $(\text{SN})_x$  has a higher work function than elemental metals [81]. Cohen and Harris [82] have taken advantage of this to enhance the open circuit voltage of GaAs solar cells. Polyacetylene has also been shown to form Schottky barriers [160,192] and heterojunctions [51]. Tskukamoto *et al.* [193] have fabricated Schottky barrier type solar cells using HCl doped  $(\text{CH})_x$  as the semiconductive element. The energy efficiency is about 0.2%. Pristine  $(\text{CH})_x$  has been used as the photoelectrode in a photochemical photovoltaic cell [161].

In addition to their use in the role of classical semiconductors and metals, challenging established materials in established technologies, conducting polymers offer additional technological opportunities which take advantage of their unique properties. The electroactive properties of the polypyrroles and  $(\text{CH})_x$  have been explored, and it has shown that these materials can be repeatedly electrically switched between the metallic and the insulating states - a change which can be followed optically as well as electrically [183]. The large surface area of polyacetylene ( $60 \text{ m}^2\text{g}^{-1}$ ) [194] and the fact that the

fibrils can be covered with finely divided silver metal [55] suggest possible catalytic applications. It is also possible that replacing carbon loaded "conducting" polymers with intrinsically conducting polymers would lead to superior performance, avoiding the problems of high frequency cut-off and high field breakdown associated with the carbon particles.

The metallic properties of conducting polymers permit them to be utilized as electrode materials. Nowak *et al.* [195] have shown that  $(SN)_x$  has good electrode characteristics, and Diaz *et al.* [183] have shown that polypyrrole tetrafluoroborate forms a stable nonporous electrode. Noufi *et al.* [57] have used polypyrrole as a passivating layer to prevent dissolution of n-GaAs photoanodes in a photochemical solar cell.

Exciting as the above outlined prospects may be, it is important to recognize the problems that must be solved before conducting polymers can find widespread technological application.

From the discussion of the magnitude of the conductivities of presently known conducting polymers (except perhaps  $AsF_5$ -treated graphite), it is obvious that these materials will not displace copper or the classical metals. In most applications, if they are to become practical materials rather than laboratory curiosities, their usefulness will most probably be found in a rather unique blend of their electronic, mechanical and processing characteristics. Indeed, conducting polymers are probably best considered not as competitors for the classical metals or semimetals, but as materials providing new opportunities due to the incorporation into conducting materials of such attractive polymer properties as melt and solution processibilities, low density and plasticity or elasticity.

Ideally, these polymers would also satisfy a variety of increasingly important ecological considerations such as low toxicity and nonenergy-intensive synthesis and processing. Preparation from nonpolluting aqueous media would, of course, be desirable. Advantage could also conceivably follow from the thermal conductivities and high absorption coefficients of these metallic polymers.

Though some of these properties, such as low density and high absorption coefficient, characterize all of the existing conducting polymers, some of the other desirable properties described here are not typical of either  $(SN)_x$  or the chemically (as opposed to electrochemically) modified systems. In particular, neither  $(SN)_x$  nor the chemically modified conducting polymers are stable in air (particularly the alkali metal reduced n-type polymers), nor are they thermally stable much above room temperature. The majority of dopants used to impart conductivity to the polymers (e.g.,  $AsF_5$ ,  $I_2$ ,  $Br_2$ , etc.) are highly toxic. In addition, the chemical doping process universally appears to degrade the mechanical properties of these polymers, making them brittle where previously they were flexible. In contrast to the chemically oxidized systems, electrochemically oxidized polypyrrole- $BF_4$ , after initial air oxidation, is stable in air for several months, though its electrical conductivity slowly decreases, and shows appreciable thermal stability, though its flexibility is not yet ideal. Some of the copolymer films of acetylene and methylacetylene reported by Karasz and coworkers have exhibited elastic properties when wet with solvent [23]. When dry these films are relatively brittle but on wetting again with solvent they can be readily stretched and retain their elongation if dried under tension.

Obviously there will be certain applications such as batteries where the conducting polymer system can be maintained in a restricted atmosphere and considerations of air stability and flexibility are not crucial. However, for widespread applications, taking full advantage of these materials, a significant amount of polymer engineering will be necessary to stabilize these materials and improve their polymeric properties in the metallic and semiconducting state. The increasingly wide variety and complexity of polymers which can be made to show high conductivity bodes well for the ability of scientists to incorporate these desirable properties into such materials.

#### ACKNOWLEDGMENTS

We would like to thank the Office of Naval Research for partial support of this work.

## REFERENCES

1. A. J. Berlinsky, Contemporary Physics 17, 331 (1976).
2. H. R. Zeller, in Festkörper Probleme XIII, Advances in Solid State Physics, Pergamon Press, Vieweg, 1973, p. 31.
3. Highly Conducting One-Dimensional Solids (Devreese, Evrard and van Doren, eds.), Plenum Press, New York.
4. D. Chapman, R. J. Warn, A. G. Fitzgerald and A. D. Yoffe, 1980, Trans. Far. Soc. 60, 294 (1964).
5. V. V. Walatka, M. M. Labes and J. H. Perlstein, Phys. Rev. Lett. 31, 1139 (1973).
6. R. L. Greene, G. B. Street and L. J. Suter, Phys. Rev. Lett. 34, 577 (1975).
7. C. Bernard, A. Herold, M. Lelaurain and G. Robert, C. R. Acad. Sci. C283, 125 (1976).
8. G. B. Street, W. D. Gill, R. H. Geiss, R. L. Greene and J. J. Mayerle, J.C.S. Chem. Commun. 407 (1977).
9. W. D. Gill, W. Bludau, R. H. Geiss, P. M. Grant, R. L. Greene, J. J. Mayerle and G. B. Street, Phys. Rev. Lett. 38, 1305 (1977).
10. M. Akhtar, J. Kleppinger, A. G. MacDiarmid, J. Milliken, M. J. Cohen, A. J. Heeger and D. L. Peebles, J.C.S. Chem. Commun. 473 (1977).
11. C. K. Chiang, M. J. Cohen, D. L. Peebles, A. J. Heeger, M. Akhtar, J. Kleppinger, A. G. MacDiarmid, J. Milliken and M. J. Moran, Solid State Commun. 23, 607 (1977).
12. H. C. Longuet-Higgins and L. Salem, Proc. Roy. Soc. (London) A251, 172 (1959); M. Tsuji, S. Huzinaga and T. Hasino, Rev. Mod. Phys. 32, 425 (1960); 557 (1971); J. E. Falk and R. J. Fleming, J. Phys. C8, 627 (1975).

13. G. Natta, G. Mazzanti and P. Corradini, Att. Acad. Nazl. Lincei, Rend. Classe Sci. Fis. Mat. Nat. 15, 3 (1958).
14. D. J. Berets and D. S. Smith, Trans. Far. Soc. 64, 827 (1968).
15. I. Ito, H. Shirakawa and S. Ikeda, J. Polym. Sci., Polym. Chem. Ed. 12, 11 (1974).
16. C. K. Chiang, C. R. Fincher, Jr., Y. W. Parks, A. J. Heeger, H. Shirakawa, E. J. Louis, S. C. Gau and A. G. MacDiarmid, Phys. Rev. Lett. 39, 1098 (1977).
17. G. B. Street and T. C. Clarke, IBM J. Res. and Develop. 25, 51 (1981).
18. F. P. Burt, J. Chem. Soc. 1121 (1910).
19. R. D. Smith, J.C.S. Dalton Trans., 478 (1979).
20. M. Goehring and D. Voigt, Naturwissenschaften 40, 482 (1953).
21. M. J. Cohen, A. F. Garito, A. J. Heeger, A. G. MacDiarmid, C. M. Mikulski and M. S. Saran, J. Amer. Chem. Soc. 98, 3844 (1975).
22. R. H. Baughman, R. R. Chance and M. J. Cohen, J. Chem. Phys. 64, 1869 (1976).
23. G. B. Street, H. Arnal, W. D. Gill, P. M. Grant and R. L. Greene, Mater. Res. Bull. 10, 877 (1475).
24. C. M. Mikulski, P. J. Russo, M. S. Saran, A. G. MacDiarmid, A. F. Garito and A. J. Heeger, J. Amer. Chem. Soc. 97, 6358 (1975).
25. H. Kahlert and B. Kundu, Mat. Res. Bull. 11, 967 (1976).
26. M. M. Labes, P. Love and L. F. Nichols, Chemical Reviews 79, 1 (1979).
27. P. Love, H. I. Kao, G. H. Myer and M. M. Labes, J.C.S. Chem. Commun. 301 (1978).
28. R. L. Patton, Ph.D. Thesis, University of California, Berkeley, 1969.
29. C. Hsu and M. M. Labes, J. Chem. Phys. 61, 4640 (1974).

30. E. J. Louis, A. G. MacDiarmid, A. F. Garito and A. J. Heeger, J.C.S. Chem. Commun. 426 (1976).
31. A. A. Bright, M. J. Cohen, A. F. Garito, A. J. Heeger, C. M. Mikulski and A. G. MacDiarmid, Appl. Phys. Lett. 26, 612 (1975).
32. R. D. Smith, J. R. Wyatt, D. Weber, J. J. DeCorpo and F. E. Saalfeld, Inorg. Chem. 17, 1639 (1978).
33. R. A. Teichman and E. R. Nixon, Inorg. Chem. 15, 1993 (1976).
34. W. Beyer, W. D. Gill and G. B. Street, Solid State Commun. 27, 343 (1978).
35. W. Beyer, H. Mell and W. D. Gill, Solid State Commun. 27, 185 (1978).
36. R. D. Smith, J. R. Wyatt, J. J. DeCorpo, F. E. Saalfeld, M. J. Moran and A. G. MacDiarmid, Chem. Phys. Lett. 41, 362 (1976).
37. F. E. Saalfeld, J. J. DeCorpo, J. R. Wyatt, P. T. Mah and W. N. Allen, Ann. N.Y. Acad. Sci. 313, 759 (1978).
38. R. R. Cavanagh, R. S. Altman, D. R. Herschbach and W. Klemperer, JACS 101, 4734 (1979).
39. Z. Iqbal and D. S. Downs, Chem. Phys. 44, 137 (1979).
40. H. Ishida, S. E. Rickert, A. J. Hopfinger, J. B. Lando, E. Baer and J. L. Koenig, J. Appl. Phys. 51, 5188 (1980).
41. H. Nishiharg, I. Nakada and K. Satoh, submitted to J. Phys. Chem. Solids (1981).
42. M. Seel, T. C. Collin, F. Martino, D. K. Rai and J. Ladik, Phys. Rev. B 18, 6460 (1978).
43. M. Goehring and D. Voigt, Z. Anorg. Allg. Chem. 285, 181 (1956).
44. A. Douillard, Ph.D. Thesis, Claude Bernard University, Lyon, France (1972).
45. M. Boudeulle, Crystal Structure Commun. 4, 9 (1975).

46. G. Heger, S. Klein, L. Pintschovious and H. Kahlert, J. Solid State Chem. 23, 341 (1978).
47. (a) H. J. Stoltz, A. Otto and L. Pintschovius, Proc. III Internat. Conf. on Light Scattering Solids, Campinas, Brazil, July 1975, edited by M. Balkanski, R. C. C. Leite and S. P. S. Porto (Flammarion Sciences, Paris, 1976), p. 736; (b) H. J. Stoltz, H. Wendel, A. Otto, L. Pintschovius and H. Kahlert, Phys. Stat. Sol. (b) 78, 277 (1976).
48. H. Temkin and D. B. Fitchen, Solid State Commun. 19, 1181 (1976).
49. H. Wendel, J. Phys. C 10, L1 (1977).
50. (a) Z. Iqbal, R. H. Baughman, J. Kleppinger and A. G. MacDiarmid, Ann. N.Y. Acad. Sci. 313, 775 (1978); (b) Z. Iqbal, R. H. Baughman, J. Kleppinger and A. G. MacDiarmid, Solid State Commun. 25, 469 (1978).
51. See references in the following reviews; R. L. Greene and G. B. Street, in Chemistry and Physics of One-Dimensional Metals (H. J. Keller, ed.), Plenum Publishing Corp., New York, 1977, p. 167; H. P. Geserich and L. Pintschovius, in Advances in Solid State Physics, Vol. XVI (J. Treusch, ed.), Vieweg, Braunschweig, 1976, p. 65; G. B. Street and W. D. Gill, in Molecular Metals (W. E. Hatfield, ed.), Plenum Publishing Corp., New York, 1979, p. 301.
52. D. E. Parry and J. M. Thomas, J. Phys. C 8, L45 (1975).
53. P. M. Grant, R. L. Greene and G. B. Street, Phys. Rev. Lett. 35, 1743 (1975).
54. C. H. Chen, J. Silcox, A. F. Garito, A. J. Heeger and A. G. MacDiarmid, Phys. Rev. Lett. 36, 525 (1976).
55. W. E. Rudge and P. M. Grant, Phys. Rev. Lett. 35, 1799 (1975).

56. P. M. Grant, W. E. Rudge and I. B. Ortenburger, Lecture Notes in Physics, Vol. 165, Organic Conductors and Semiconductors, Springer-Verlag, Berlin (1977).
57. G. B. Street and R. L. Greene, IBM J. Res. and Develop. 21, 99 (1977).
58. C. K. Chiang, M. J. Cohen, A. F. Garito, A. J. Heeger, C. M. Mikulski and A. G. MacDiarmid, Solid State Commun. 18, 1451 (1976).
59. W. D. Gill, R. L. Greene, G. B. Street and W. A. Little, Phys. Rev. Lett. 35, 1732 (1975).
60. G. B. Street and W. D. Gill, in Molecular Metals (W. H. Hatfield, ed.), Plenum Publishing Corp., New York, 1979, p. 301.
61. R. H. Dee, A. J. Berlinsky, J. F. Carolan, E. Klein, N. J. Stone, B. G. Turrell and G. B. Street, Solid State Commun. 23, 303 (1977).
62. L. F. Lou and A. F. Garito, unpublished, see Figure 12 in R. L. Greene and G. B. Street, Ref. 15.
63. R. H. Dee, D. H. Dollard, B. G. Turrell and J. F. Carolan, Solid State Commun. 24, 469 (1977).
64. Y. Oda, H. Takenaka, H. Nagano and I. Nakada, Solid State Commun. 32, 659 (1979).
65. W. H. G. Müller, F. Baumann, G. Dammer and L. Pintschovius, Solid State Commun. 25, 119 (1978).
66. L. R. Bickford, R. L. Greene and W. D. Gill, Phys. Rev. B 17, 3525 (1978).
67. F. DeLaCruz and H. J. Stoltz, Solid State Commun. 20, 241 (1976); R. J. Soulen and D. B. Utton, Solid State Commun. 21, 105 (1977).
68. W. Beyer, W. D. Gill and G. B. Street, Solid State Commun. 27, 343 (1978).

69. C. J. Adkins, J. M. D. Thomas and M. W. Young, *J. Phys. C Solid State Phys.* 13, 3427 (1980).
70. P. M. Chaikin, P. K. Hansma and R. L. Greene, *Phys. Rev. B* 17, 179 (1978).
71. L. J. Azevedo, W. G. Clark, G. Deutscher, R. L. Greene, G. B. Street and L. J. Suter, *Solid State Commun.* 19, 197 (1976).
72. R. L. Civiak, C. Elbaum, W. Junker, C. Gough, K. I. Kao, L. F. Nichols and M. M. Labes, *Solid State Commun.* 18, 1205 (1976).
73. A. A. Bright, M. J. Cohen, A. F. Garito, A. J. Heeger, C. M. Mikulski, P. J. Russo and A. G. MacDiarmid, *Phys. Rev. Lett.* 34, 206 (1975); L. Pintschovius, H. P. Geserich and W. Möller, *Solid State Commun.* 17, 477 (1975).
74. W. Beyer, W. D. Gill and G. B. Street, *Solid State Commun.* 23, 577 (1977).
75. J. M. E. Harper, R. L. Greene, P. M. Grant and G. B. Street, *Phys. Rev. B* 15, 539 (1977); R. L. Greene, P. M. Grant and G. B. Street, *Phys. Rev. Lett.* 34, 89 (1975).
76. L. Pintschovius, H. Wendel and H. Kahlert, in Lecture Notes in Physics, Organic Conductors and Semiconductors (L. Pál, G. Grüner, A. Jánossy, J. Sólyom, eds.), Springer-Verlag, Berlin, 1977, p. 589.
77. L. Ley, *Phys. Rev. Lett.* 35, 1976 (1975); P. Mengel, P. M. Grant, W. E. Rudge, B. H. Schechtman and D. W. Rice, *Phys. Rev. Lett.* 35, 1803 (1975); W. R. Salaneck, J. W. Lin and A. J. Epstein, *Phys. Rev. B* 13, 5574 (1976).
78. E. E. Koch and W. D. Grobman, *Solid State Commun.* 23, 49 (1977); P. Mengel, I. B. Ortenburger, W. E. Rudge and P. M. Grant, in Lecture Notes in Physics, Organic Conductors and Semiconductors (L. Pál, G. Grüner, A. Jánossy, J. Sólyom, eds.), Springer-Verlag, Berlin, 1977, p. 591.

79. K. Kaneto, M. Yamamoto, K. Yoshino and Y. Inuishi, Solid State Commun. 26, 311 (1978).
80. H. Kahlert and K. Seeger, Physics of Semiconductors, Proc. 13th Int. Conf. Rome (F. G. Fumi, ed.), Tipographia Marves, Rome (1976).
81. R. A. Scranton, J. Appl. Phys. 48, 3838 (1977); R. A. Scranton, J. S. Best and J. O. McCaldin, J. Vac. Sci. Technol. 14, 930 (1977).
82. M. J. Cohen and J. S. Harnis, Jr., Appl. Phys. Lett. 33, 812 (1978).
83. V. A. Starodub, V. P. Babiuchuk, V. P. Batulin, I. V. Krivoshei and N. V. Mansya, Phys. Stat. Sol. (a) 59, K231 (1980).
84. J. Kuyper and G. B. Street, J. Amer. Chem. Soc. 99, 7848 (1977).
85. G. Wolmerhäuser and G. B. Street, Inorg. Chem. 17, 2685 (1978).
86. G. B. Street, R. L. Bingham, J. I. Crowley and J. Kuyper, J.C.S. Chem. Commun. 464 (1977).
87. M. Akhtar, C. K. Chiang, A. J. Heeger and A. G. MacDiarmid, J.C.S. Chem. Commun. 846 (1977).
88. G. B. Street, S. Etemad, R. H. Geiss, W. D. Gill, R. L. Greene and J. Kuyper, Anal. New York Acad. Sci. 313, 737 (1978).
89. H. Temkin and G. B. Street, Solid State Commun. 25, 455 (1978); H. Temkin, D. B. Fitchen, W. D. Gill and G. B. Street, New York Acad. Sci. 313, 771 (1978).
90. R. D. Smith and G. B. Street, Inorg. Chem. 17, 941 (1978).
91. M. Akhtar, C. K. Chiang, A. J. Heeger, J. Milliken and A. J. MacDiarmid, Inorg. Chem. 17, 1539 (1978).
92. J. J. Song, D. D. L. Chung, P. C. Eklund and M. S. Dresselhaus, Solid State Commun. 20, 1111 (1976).

93. J. Macklin, G. B. Street and W. D. Gill, *J. Chem. Phys.* 70, 2425 (1979).
94. H. Morawitz, W. D. Gill, P. M. Grant, G. B. Street and D. Sayers, Lecture Notes in Physics (S. Barisic *et al.*, ed.), Springer, Berlin, 1979; H. Morawitz, P. Bagus, T. Clarke, W. Gill, P. Grant and G. B. Street, *Synthetic Metals* 1, 267 (1980).
95. J. C. Scott, J. D. Kulick and G. B. Street, *Solid State Commun.* 28, 723 (1978).
96. W. N. Allen, J. J. DeCorpo, F. E. Saalfeld and J. R. Wyatt, *Chem. Phys. Lett.* 54, 524 (1978).
97. R. H. Geiss, J. Thomas and G. B. Street, *Synthetic Metals* 1, 527 (1980).
98. R. Tubino, L. Piseri, G. Carcanos and I. Pollini, *Solid State Commun.* 34, 173 (1980).
99. W. D. Gill, J. F. Kwak, R. L. Greene and G. B. Street, *Bull. Amer. Phys. Soc.* 23, 382 (1978).
100. J. F. Kwak, R. L. Greene and G. B. Street, *Bull. Amer. Phys. Soc.* 23, 384 (1978).
101. A. Philipp and K. Seeger, *Phys. Stat. Sol. (b)* 89, 187 (1978).
102. M. Hatano and S. Kambara, *J. Polym. Sci.* 51, S26 (1961).
103. H. Shirakawa and S. Ikeda, *Polym. J.* 2, 231 (1971).
104. R. H. Baughman, S. L. Hsu, G. P. Pez and A. J. Signorelli, *J. Chem. Phys.* 58, 5405 (1978).
105. H. Shuakawa and S. Ikeda, *Synthetic Metals* 1, 175 (1980).
106. Y. W. Park, M. A. Druy, C. K. Chiang, A. G. MacDiarmid, A. J. Heeger, H. Shirakawa and S. Ikeda, *J. Polym. Sci., Polym. Lett.* 17, 195 (1979).
107. C. R. Fincher, Jr., D. L. Pebbles, A. J. heeger, M. A. Druy, Y. Matsamura, A. G. MacDiarmid, H. Shirakawa and S. Ikeda, *Solid State Commun.* 27, 489 (1978).

108. G. W. Wnek, J. C. W. Chien, M. A. Druy, Y. W. Park, A. G. MacDiarmid and A. J. Heeger, *J. Polym. Sci., Polym. Lett. Ed.* 17, 779 (1979).
109. G. Lieser, G. Wegner, W. Müller and V. Enkelmann, *Makromol. Chem., Rapid Commun.* 1, 621 (1980).
110. J. H. Edwards and W. J. Feast, *Polym.* 21, 595 (1980).
111. T. Ito, H. Shirakawa and S. Ikeda, *J. Polym. Sci., Polym. Chem. Ed.* 13, 1943 (1975).
112. T. Akaishi, K. Miyasaka, K. Ishikawa, H. Shirakawa and S. Ikeda, *J. Polym. Sci., Polym. Phys. Ed.* 18, 745 (1980).
113. R. H. Baughman and S. L. Hsu, *J. Polym. Sci., Polym. Lett. Ed.* 17, 185 (1979).
114. R. H. Baughman, S. L. Hsu, L. R. Anderson, G. P. Pez and A. J. Signorelli, in *Molecular Metals*, W. E. Hatfield (ed.), Plenum Press, 1979, 183.
115. T. C. Clarke, R. H. Geiss, W. D. Gill, P. M. Grant, H. Morawitz, G. B. Street and D. E. Sayers, *Synthetic Metals* 1, 21 (1979).
116. G. Lieser, G. Wegner, W. Müller, V. Enkelmann and W. H. Meyer, *Makromol. Chem., Rapid Commun.* 1, 627 (1980).
117. K. Shimamura, F. E. Karasz, J. A. Hirsch and J. C. W. Chien, submitted for publication.
118. M. M. Maricq, J. S. Waugh, A. G. MacDiarmid, H. Shirakawa and A. J. Heeger, *J. Amer. Chem. Soc.* 100, 7729 (1978).
119. P. Bernier, F. Schue, J. Sledz, M. Rolland and L. Giral, *Chem. Scripta* 17, 151 (1981).
120. C. K. Chiang, C. R. Fincher, Jr., J. W. Park, A. J. Heeger, H. Shirakawa, E. J. Louis, S. C. Gau and A. G. MacDiarmid, *Phys. Rev. Lett.* 39, 1098 (1977).

121. J. F. Kwak, T. C. Clarke, G. B. Street and R. L. Greene, *Solid State Commun.* 31, 355 (1979).
122. K. Seeger, W. F. Gill, T. C. Clarke and G. B. Street, *Solid State Commun.* 28, 873 (1978).
123. C. K. Chiang, S. C. Gau, C. R. Fincher, Jr., Y. W. Park, A. G. MacDiarmid and A. J. Heeger, *Appl. Phys. Lett.* 33, 18 (1978).
124. T. C. Clarke and G. B. Street, "The Chemical Nature of Polyacetylene Doping," *Synthetic Metals* 1, 119 (1980).
125. P. J. Nigrey, A. G. MacDiarmid and A. J. Heeger, *J. Chem. Soc., Chem. Commun.* 594 (1979).
126. D. J. MacInnes, M. A. Druy, P. J. Nigrey, D. P. Nairns, A. G. MacDiarmid and A. J. Heeger, *J. Chem. Soc., Chem. Commun.* 317 (1981).
127. S. L. Hsu, A. J. Signorelli, G. P. Pez and R. H. Baughman, *J. Chem. Phys.* 68, 106 (1978).
128. G. B. Street and T. C. Clarke, *ACS Adv. Chem.* 186, 177 (1980).
129. S. C. Gau, J. Millikan, A. Pron, A. G. MacDiarmid and A. J. Heeger, *J. Chem. Soc., Chem. Commun.* 662 (1979).
130. T. C. Clarke, unpublished results.
131. B. W. McQuillan, G. B. Street and T. C. Clarke, to appear in *J. of Electronic Materials*; T. C. Clarke, B. W. McQuillian, J. F. Rabolt, J. C. Scott and G. B. Street, to appear in *Mol. Cryst. Liq. Cryst.*
132. T. C. Clarke, M. T. Krounbi, V. Y. Lee and G. B. Street, *J. Chem. Soc., Chem. Commun.* 384 (1981).
133. C. Rebbi, *Sci. Amer.* 240, 92 (1979).
134. J. A. Pople and S. H. Walmsley, *Mol. Phys.* 5, 15 (1962).

135. M. Nechtschein, J. Polym. Sci., Part C 4, 1367 (1963).
136. M. J. Rice, Phys. Lett. 71A, 152 (1979).
137. W. P. Su, J. R. Schrieffer and A. J. Heeger, Phys. Rev. Lett. 42, 1698 (1979).
138. P. Bernier, M. Rolland, C. Linaya and M. Disi, Polym. 21, 7 (1980).
139. H. Shirakawa, T. Ito and S. Ikeda, Makromol. Chem. 179, 1565 (1978).
140. K. Holczer, J. P. Boucher, F. Devreux and M. Nechtschein, Phys. Rev. B 23, 1051 (1981).
141. M. Nechtschein, F. Devreux, R. L. Greene, T. C. Clarke and G. B. Street, Phys. Rev. Lett. 44, 356 (1980).
142. N. S. Shiren, Y. Tomkiewicz, T. G. Kazyaka, A. R. Taranko, H. Thomann, L. Dalton and T. C. Clarke, Phys. Rev. Lett., submitted.
143. S. Etemad, K. B. Lee, T.-C. Chung, A. J. Heeger, A. G. MacDiarmid, B. R. Weinberger and S. C. Gau, to be published.
144. L. Lauchlan, S. Etemad, T.-C. Chung, A. J. Heeger and A. G. MacDiarmid, to be published.
145. S. Ikehata, J. Kaufer, T. Woerner, A. Pron, M. A. Pruy, A. Sivak, A. J. Heeger and A. G. MacDiarmid, Phys. Rev. Lett. 45, 1123 (1980).
146. Y. Tomkiewicz, T. D. Schultz, H. B. Brom, T. C. Clarke and G. B. Street, Phys. Rev. Lett. 43, 1532 (1979).
147. Y. Tomkiewicz, T. D. Schultz, H. B. Brom, A. R. Taranko, T. C. Clarke and G. B. Street, Phys. Rev. B, in press.
148. G. Grüner and A. Zettler, unpublished results.
149. M. Mortensen, M. L. W. Thewalt, Y. Tomkiewicz, T. C. Clarke and G. B. Street, Phys. Rev. Lett. 45, 490 (1980).

150. T. C. Clarke, M. A. Druy, J. Flood, A. J. Heeger, S. Ikehata, A. G. MacDiarmid, A. R. Taranko, Y. Tomkiewicz and T. Woerner, unpublished results.
151. M. Peo, H. Förster, K. Menke, J. Hocker, J. A. Gardner, S. Roth and K. Dransfeld, Solid State Commun. 38, 467 (1981).
152. T. C. Clarke and J. C. Scott, Solid State Commun., submitted.
153. E. J. Mele and M. J. Rice, Solid State Commun. 34, 339 (1980).
154. C. R. Fincher, Jr., M. Ozaki, A. H. Heeger and A. G. MacDiarmid, Phys. Rev. B 19, 4140 (1979); S. Etemad, A. Pron, A. J. Heeger, A. G. MacDiarmid, F. J. Mele and M. J. Rice, Phys. Rev. B 23, 5137 (1981).
155. J. F. Rabolt, T. C. Clarke and G. B. Street. J. Chem. Phys. 71, 4614 (1979); J. F. Rabolt, T. C. Clarke and G. B. Street, unpublished results.
156. P. M. Grant and I. P. Batra, Solid State Commun. 29, 225 (1979).
157. R. V. Kasowski, W. Y. Hsu and E. Caruthers, J. Chem. Phys. 72, 4896 (1980).
158. T. Yanabe, K. Tanaka, H. Terama-e, K. Fukui, A. Imamura, H. Shirakawa and S. Ikeda, Solid State Commun. 29, 329 (1979).
159. R. V. Kasowski, E. Caruthers and W. Y. Hsu, Phys. Rev. Lett. 44, 676 (1980).
160. T. Tani, W. D. Gill, P. M. Grant, T. C. Clarke and G. B. Street, Synthetic Metals 1, 301 (1980); Solid State Commun. 33, 499 (1980).
161. S. N. Chen, A. J. Heeger, Z. Kiss, A. G. MacDiarmid, S. C. Gau and D. L. Peebles, Appl. Phys. Lett. 36, 96 (1980).
162. Y. W. Park, A. J. Heeger, M. A. Druy and A. G. MacDiarmid, J. Chem. Phys. 73, 946 (1980).
163. Y. W. Park, A. Denenstein, C. K. Chiang, A. J. Heeger and A. G. MacDiarmid, Solid State Commun. 29, 747 (1979).

164. J. F. Kwak, W. D. Gill, R. L. Greene, K. Seeger, T. C. Clarke and G. B. Street, *Synthetic Metals* 1, 213 (1980).
165. M. Ozaki, D. L. Peebles, B. R. Weinberger, C. K. Chiang, S. C. Gau, A. J. Heeger and A. G. MacDiarmid, *Appl. Phys. Lett.* 35, 83 (1979).
166. T. Tani, W. D. Gill, P. M. Grant, M. Krounbi, T. C. Clarke and G. B. Street, *J. Appl. Phys.* 52, 869 (1981).
167. J. C. W. Chien and F. E. Karasz, unpublished results.
168. G. M. Holob and P. Ehrlich, *J. Polym. Sci., Polym. Phys. Ed.* 15, 627 (1977); I. Diaconu, S. Dumitrescu and C. Simionescu, *Eur. Polym. J.* 15, 1155 (1979); P. Cukor, J. I. Krugler and M. F. Rubner, *Polym. Preprints* 21, 161 (1980); Y. Kuwane, T. Masuda and T. Higashimura, *Polym. J.* 12, 387 (1980).
169. J. C. W. Chien, G. E. Wnek, F. E. Karasz and J. A. Hirsch, submitted for publication.
170. H. W. Gibson, F. C. Bailey, A. J. Epstein, H. Rommelman and J. M. Pochan, *J. Chem. Soc., Chem. Commun.* 426 (1980).
171. H. W. Gibson, F. C. Bailey, J. M. Pochan, A. J. Epstein and H. Rommelman, *Electronic Materials Conference*, Ithaca, New York, 1980.
172. M. J. Kletter, T. Woerner, A. Pron, A. G. MacDiarmid, A. J. Heeger and Y. W. Park, *J. Chem. Soc., Chem. Commun.* 426 (1980).
173. T. Yamabe, K. Tanaka, H. Terama-e, K. Fukui, H. Shirakawa and S. Ikeda, *Synthetic Metals* 1, 321 (1980).
174. S. B. Maintha, P. L. Kronick, H. Ur, E. F. Chapman and M. M. Labes, *Polym. Preprints* 4, 208 (1963).
175. D. M. Ivory, G. G. Miller, J. M. Sowa, L. W. Shacklette, R. R. Chance and R. H. Baughman, *J. Chem. Phys.* 71, 1506 (1979).

176. L. W. Shacklette, H. Eckhardt, R. R. Chance, G. G. Miller, D. M. Ivory and R. H. Baughman, *J. Chem. Phys.* 73, 4098 (1980).
177. G. W. Wnek, J. C. W. Chien, F. E. Karasz and C. P. Lillya, *Polym.* 20, 1441 (1979).
178. J. F. Rabolt, T. C. Clarke, K. K. Kanazawa, J. R. Reynolds and G. B. Street, *J. Chem. Soc., Chem. Commun.* 347 (1980); T. C. Clarke, K. K. Kanazawa, V. Y. Lee, J. F. Rabolt, J. R. Reynolds and G. B. Street, *J. Polym. Sci., Polym. Phys. Ed.*, in press.
179. R. R. Chance, L. W. Shacklette, G. G. Miller, D. M. Ivory, J. M. Sowa, R. L. Elsenbaumer and R. H. Baughman, *J. Chem. Soc., Chem. Commun.* 348 (1980); L. W. Shacklette, R. L. Elsenbaumer, R. R. Chance, H. Eckhardt, J. E. Frommer and R. H. Baughman, *J. Chem. Phys.* 75, 1919 (1981).
180. Phillips Petroleum Company, Bartlesville, Oklahoma.
181. B. J. Tabor, E. P. Magré and J. Boon, *Eur. Polym. J.* 7, 1127 (1971).
182. A. F. Diaz, K. K. Kanazawa and G. P. Gardini, *J. Chem. Soc., Chem. Commun.* 635 (1979).
183. K. K. Kanazawa, A. F. Diaz, R. H. Geiss, W. D. Gill, J. F. Kwak, J. A. Logan, J. F. Rabolt and G. B. Street, *J. Chem. Soc., Chem. Commun.* 854 (1979); K. K. Kanazawa, A. F. Diaz, W. D. Gill, P. M. Grant, G. B. Street, G. P. Gardini and J. F. Kwak, *Synthetic Metals* 1, 329 (1980).
184. K. K. Kanazawa, A. F. Diaz, M. T. Krounbi and G. B. Street, *Synthetic Metals*, in press.
185. A. F. Diaz, J. I. Castillo, J. A. Logan and V. Y. Lee, submitted for publication.
186. T. Yamamoto, K. Sanechiuka and A. Yamamoto, *J. Polym. Sci., Polym. Lett. Ed.* 18, 9 (1980).

187. G. Kossmehl and G. Chatzitheodorou, *Makromol. Chem.*, in press.
188. A. F. Diaz, *Chemica Scripta* 17, 145 (1981).
189. K. F. Schoch, Jr., B. R. Kundelkar and T. J. Marks, *J. Amer. Chem. Soc.* 101, 7071 (1979); T. J. Marks, K. F. Schoch, Jr. and B. R. Kundelkar, *Synthetic Metals* 1, 337 (1980).
190. P. M. Kuznesof, K. J. Wynne, R. S. Nohr and M. E. Kenne, *J. Chem. Soc., Chem. Commun.* 121 (1980).
191. F. L. Vogel, *Synthetic Metals* 1, 274 (1980).
192. M. Ozaki, D. Peebles, B. R. Weinberger, A. J. Heeger and A. G. MacDiarmid, *J. Appl. Phys.* 51, 4252 (1980).
193. J. Tsukamoto, H. Ohigashi, K. Matsumura and A. Takashi, *Jap. J. Appl. Phys.* 20, 213 (1981).
194. A. G. MacDiarmid and A. J. Heeger, *Synthetic Metals* 1, 101 (1980).
195. R. J. Novak, H. B. Hart, A. G. MacDiarmid and D. Weber, *J. Chem. Soc., Chem. Commun.* 9 (1977).

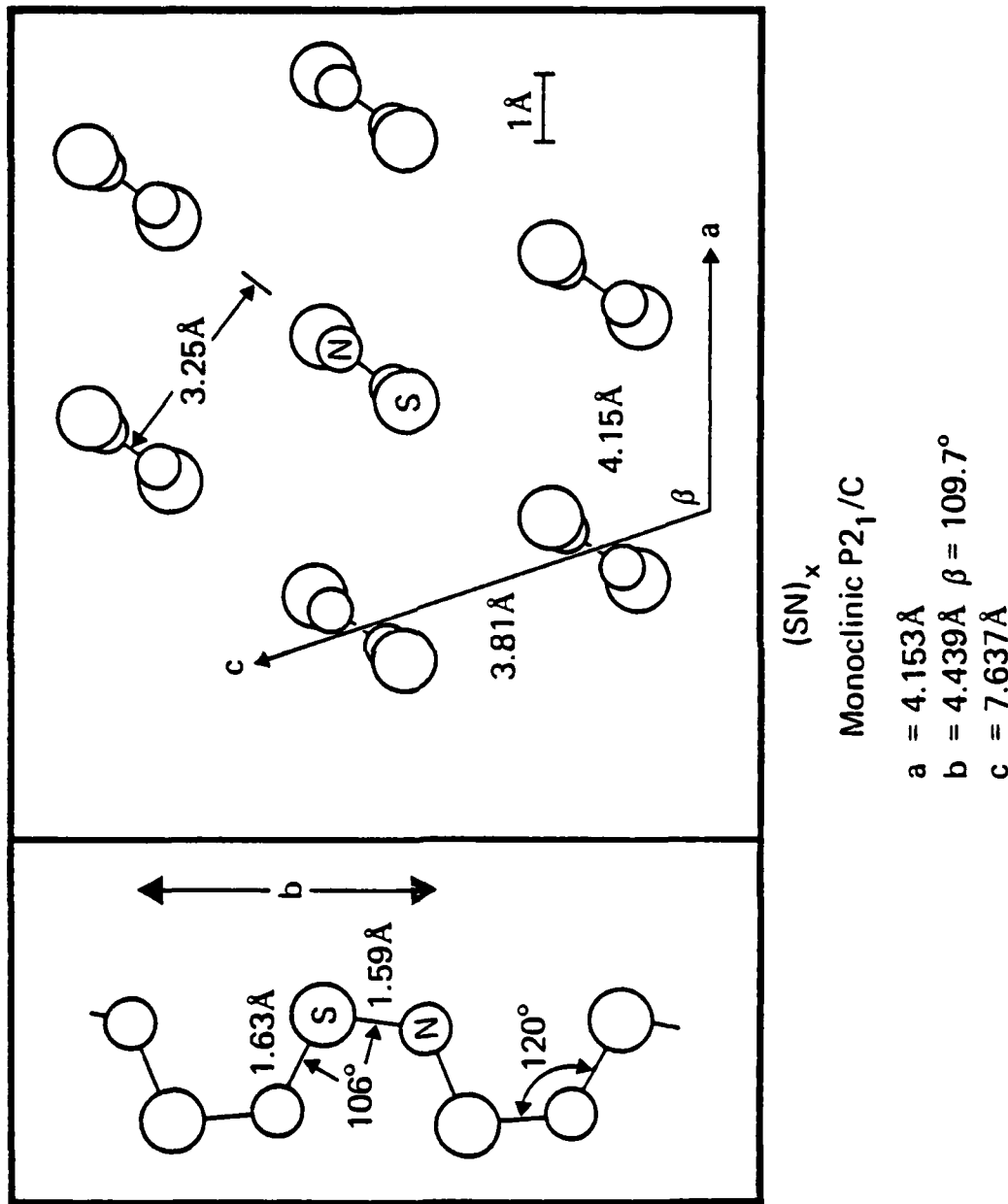


Figure 1. The structure of  $(\text{SN})_x$  crystals [21].

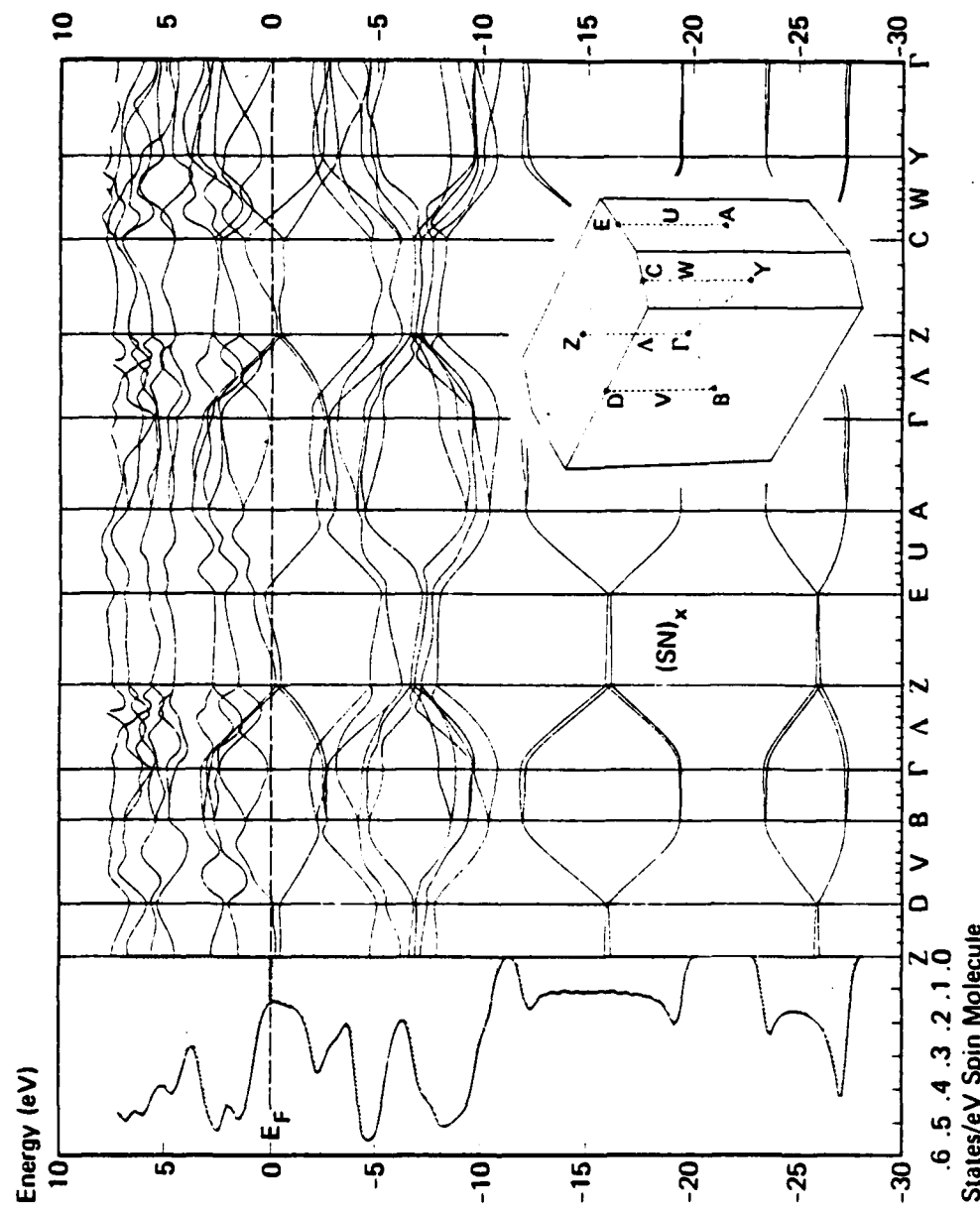


Figure 2. Band structure of  $(\text{SN})_x$  [55].

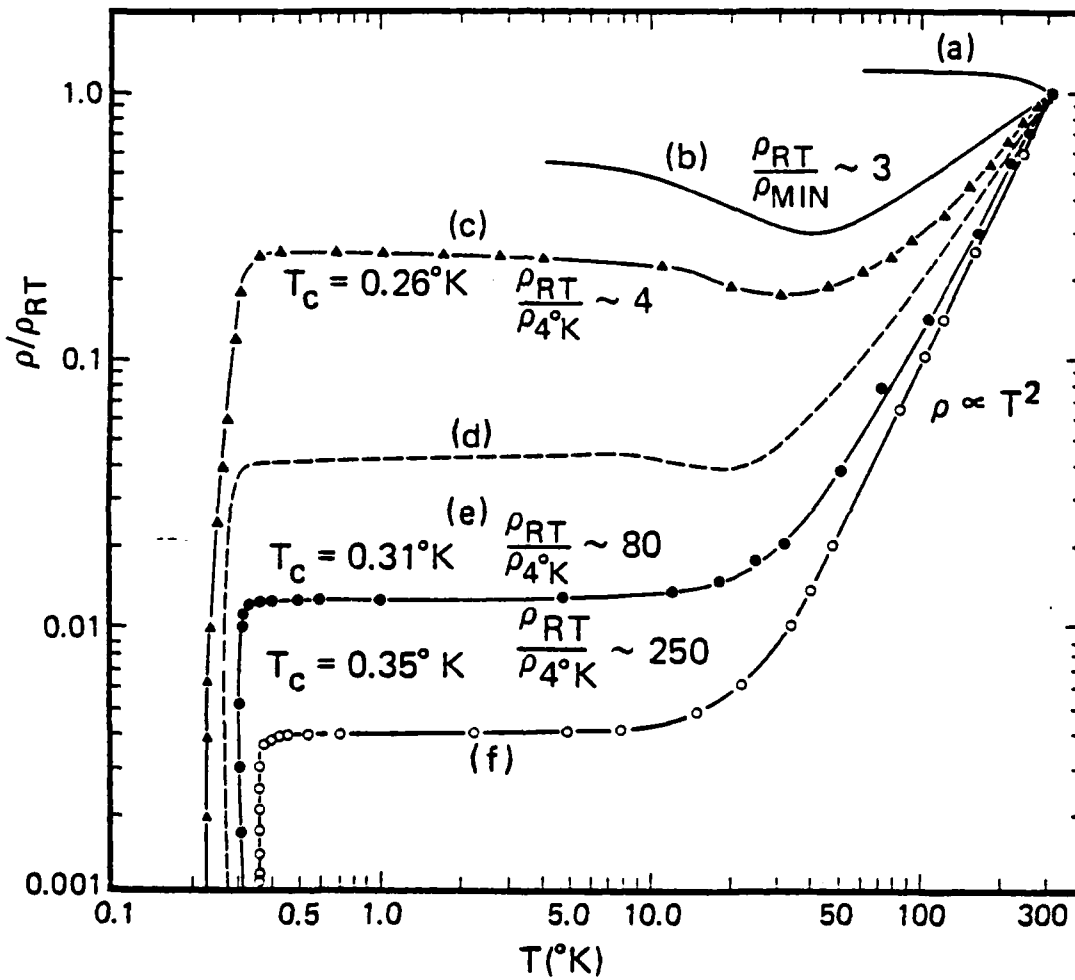


Figure 3. Temperature dependence of the resistivity of  $(\text{SN})_x$  crystals: (a)  $(\text{SN})_x$  pellets; (b) crystals from Walatka [5]; (c) crystals from Street [23]; (d),(e),(f) crystals grown by technique described by Street and Greene [57].

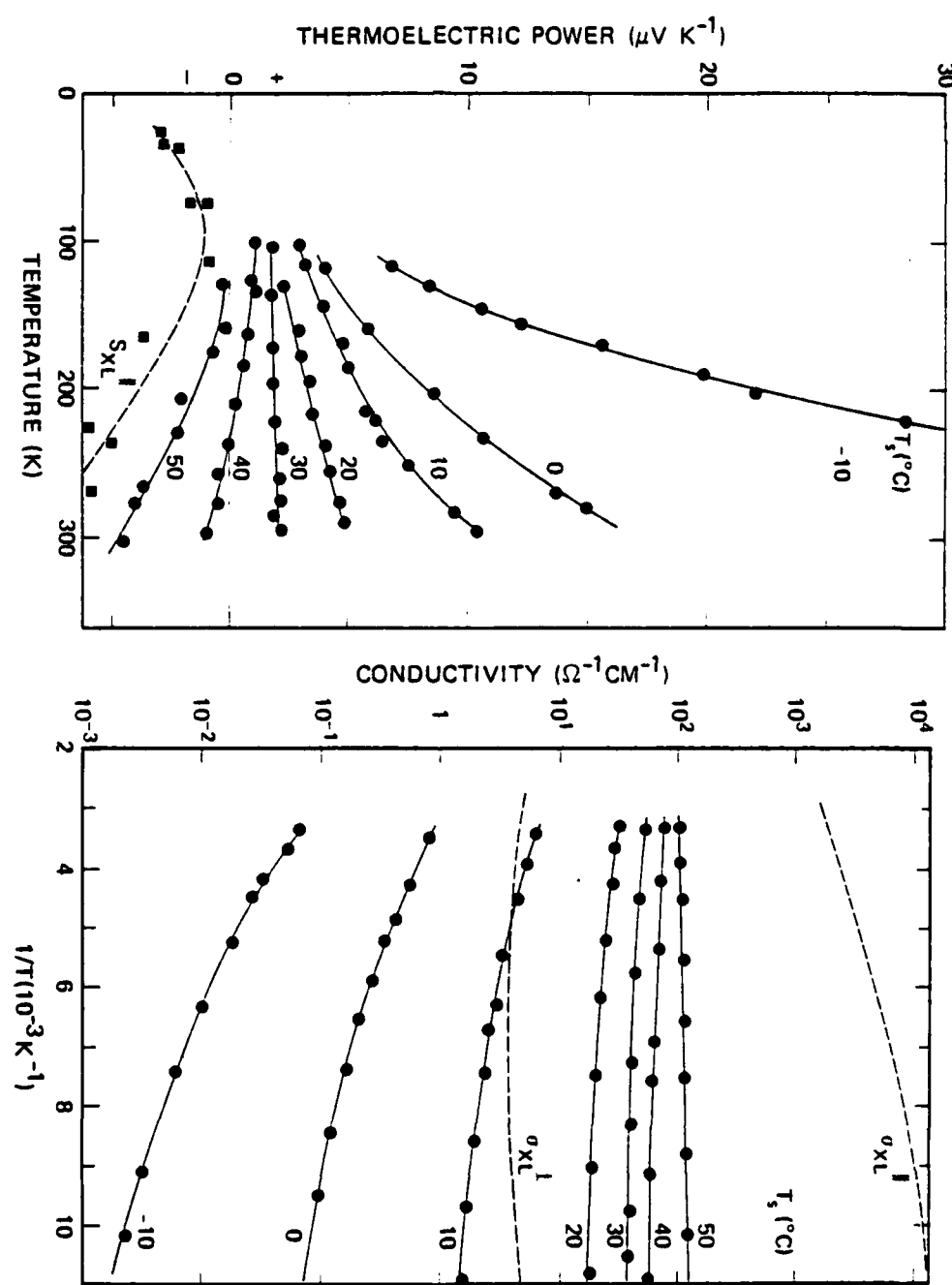


Figure 4. Temperature dependence of thermoelectric power and conductivity of  $(SN)_x$  films grown at various substrate temperatures,  $T_s$  [35,68].

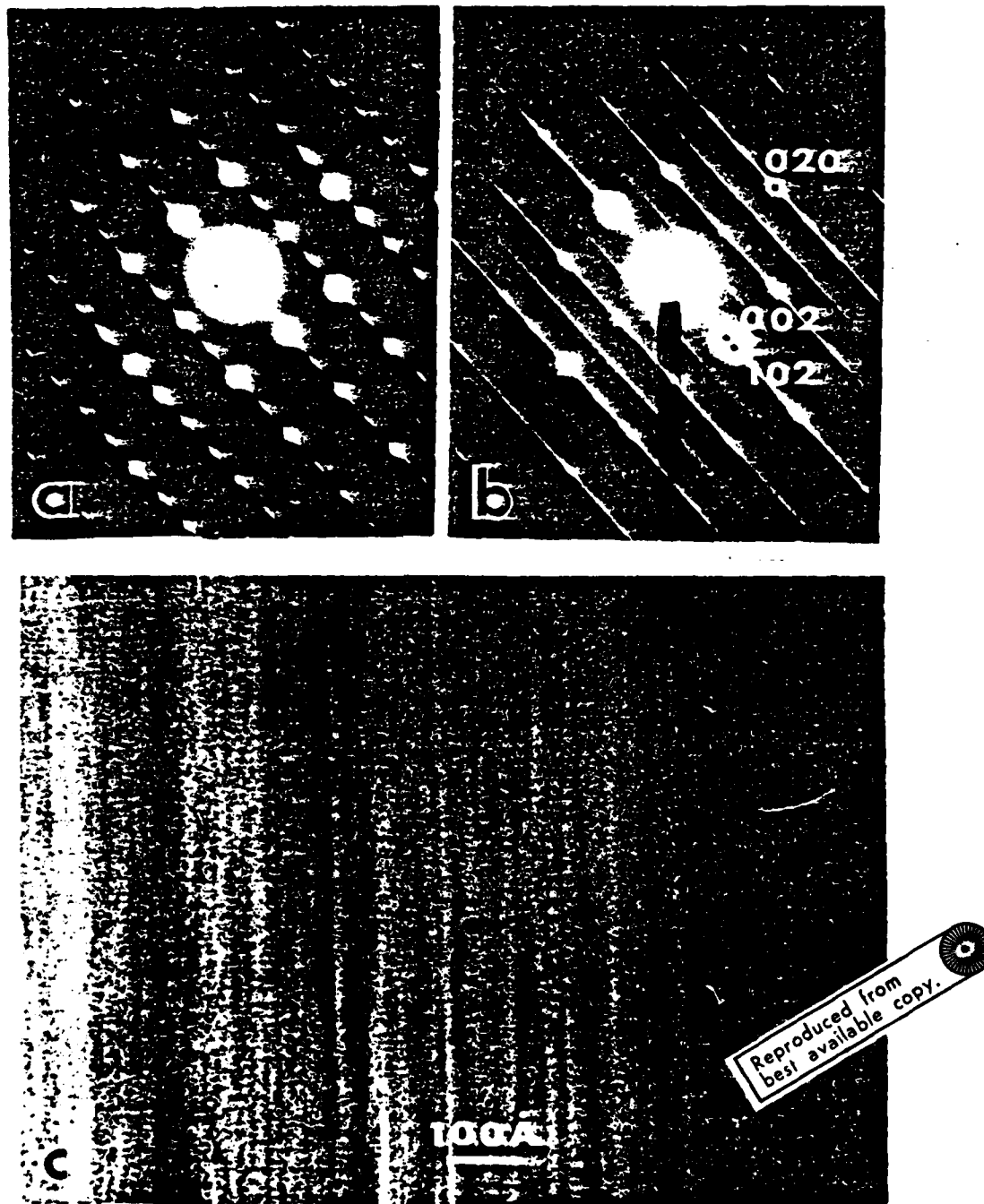


Figure 5. Electron diffraction pattern from (a)  $(SN)_x$  fibers showing the  $b^*c^*$  reciprocal lattice set; (b)  $(SNBr_{0.4})_x$  fibers oriented similarly to (a); (c) electron micrograph of  $(SNBr_{0.4})_x$  twinned fibers with 20A dimension [9].

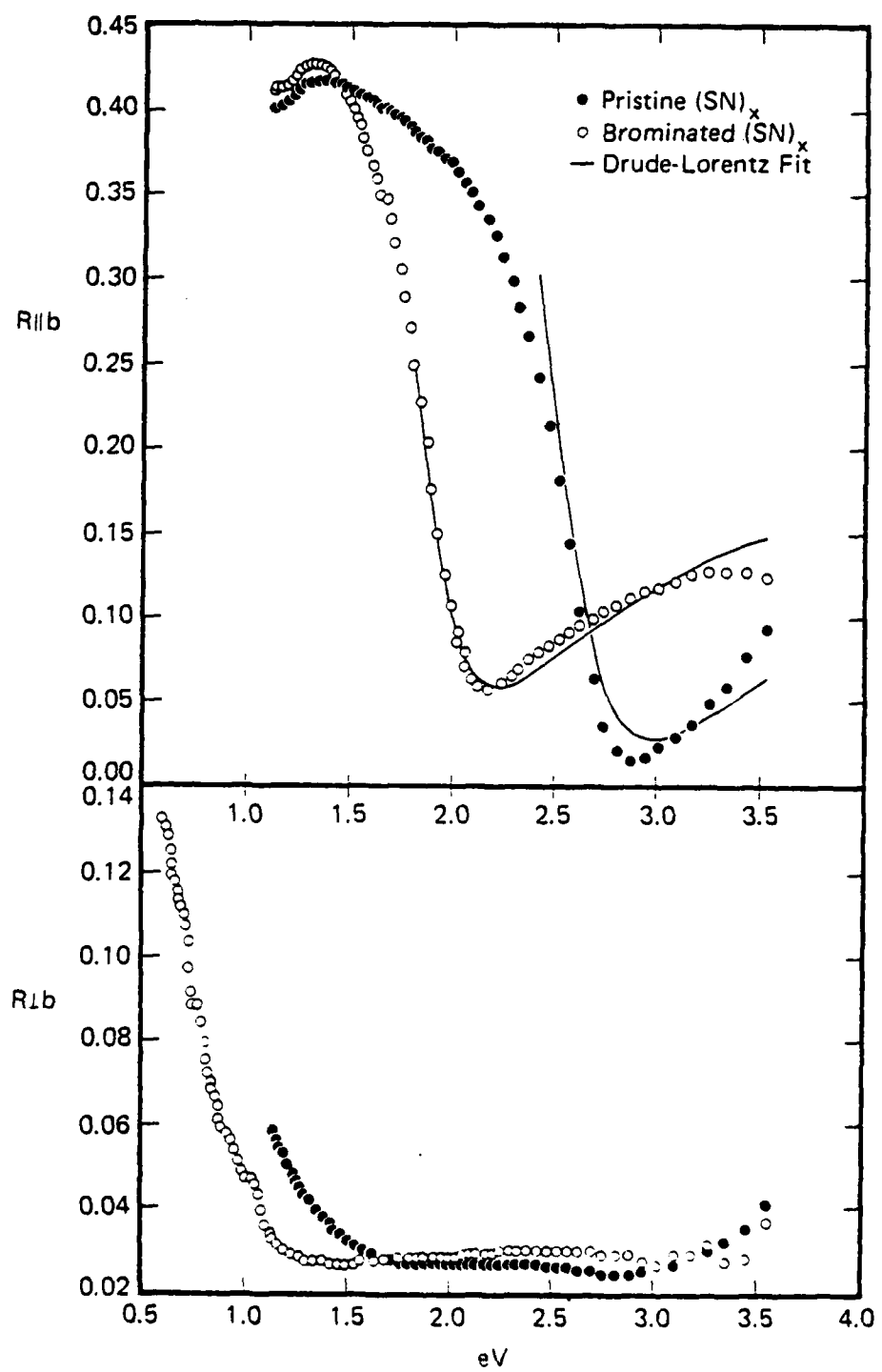


Figure 6. Polarized reflectance of the same  $(\text{SN})_x$  crystal before and after bromination [9].

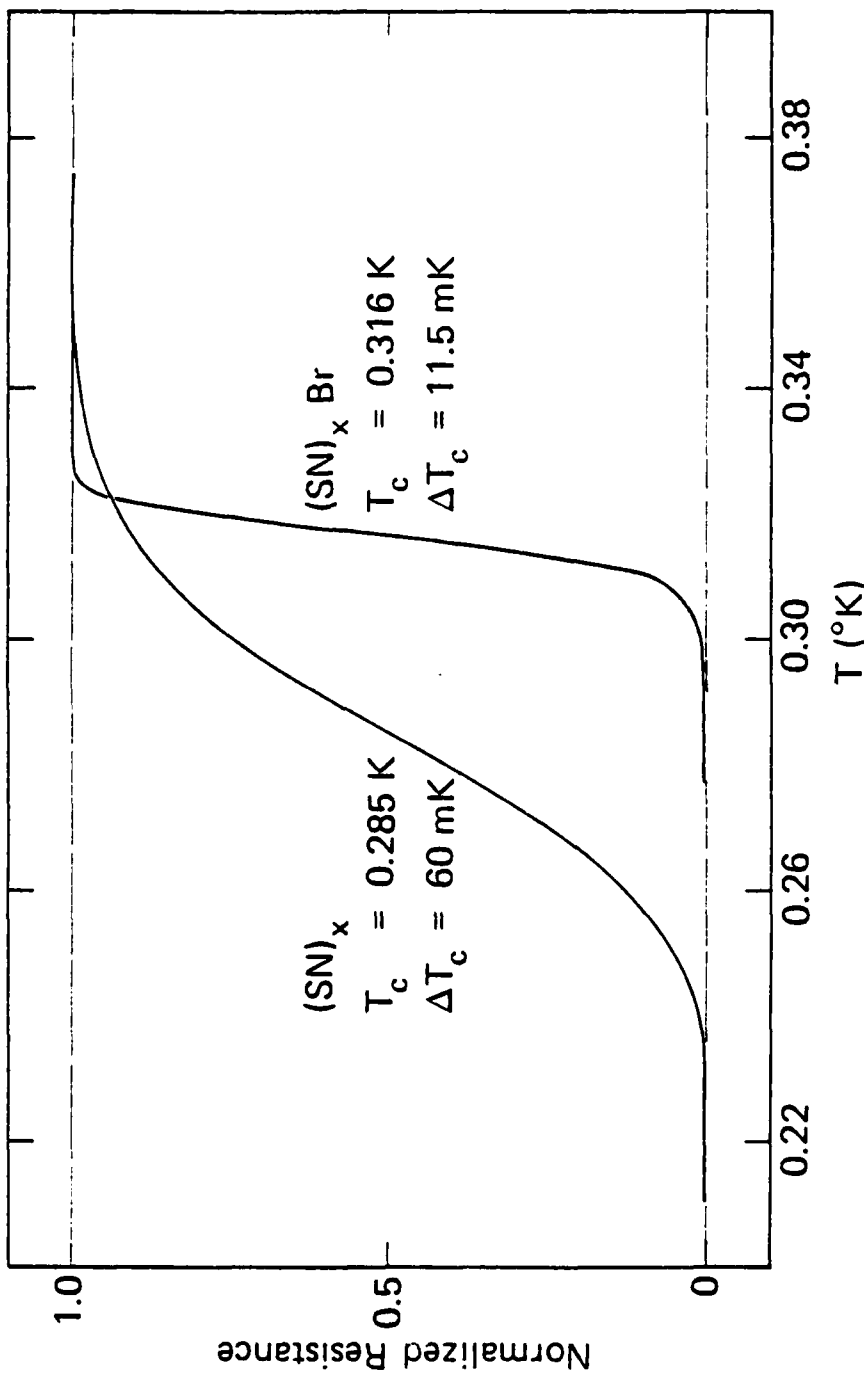


Figure 7. Superconducting transition in  $(\text{SN})_x$  and  $(\text{SNBr}_{0.4})_x$  [60].

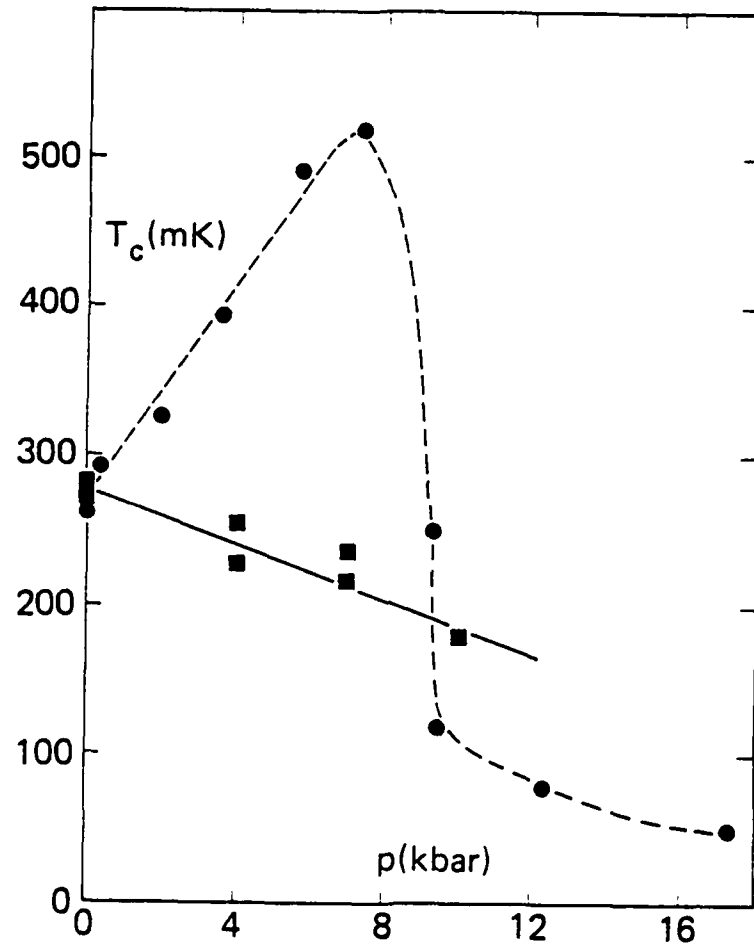


Figure 8. Pressure dependence of the superconducting transition temperature in  $(\text{SN})_x$  [60]. The  $(\text{SN})_x$  data is from Müller *et al.* [65].

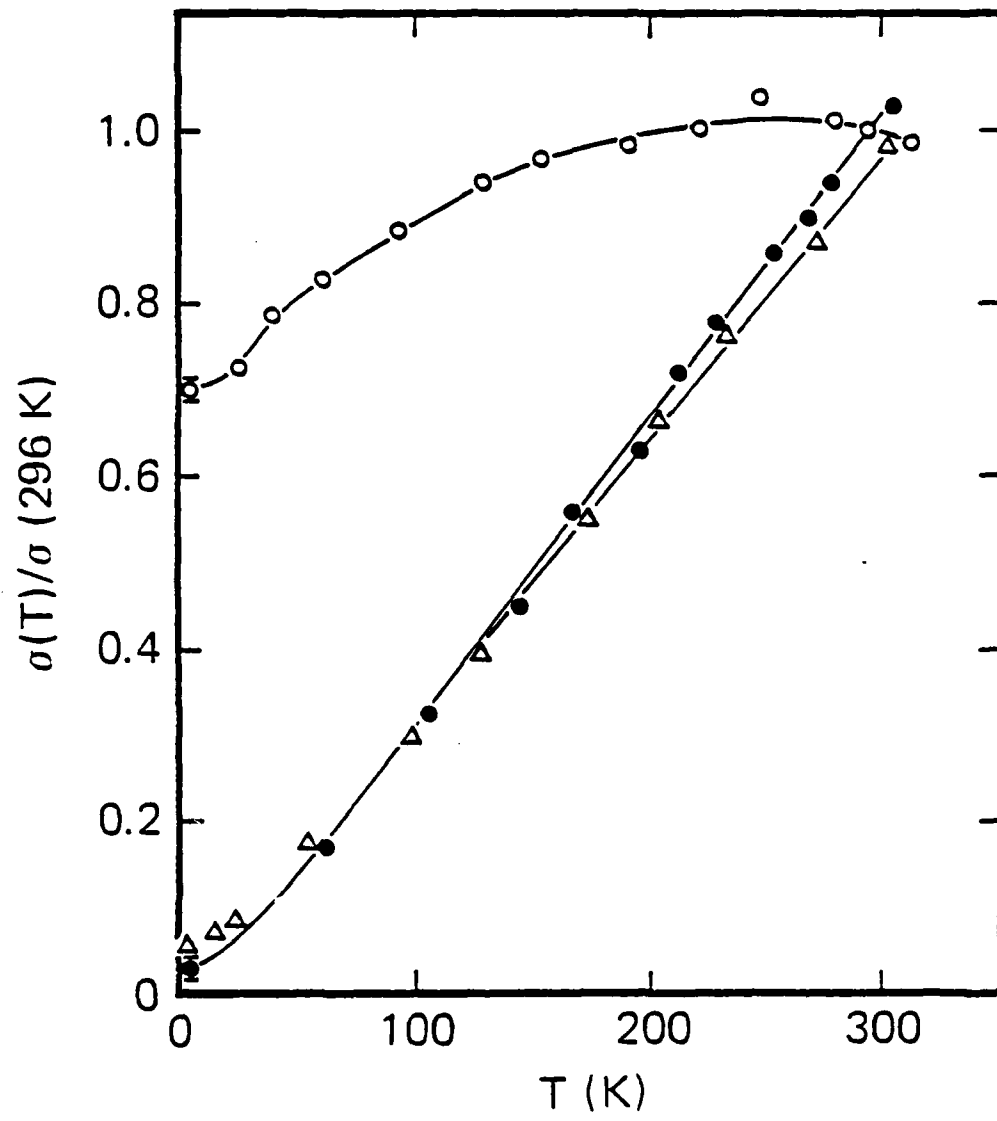


Figure 9. Temperature dependence of conductivity for intermediate and heavily doped *trans* (CH)<sub>x</sub> [122,164].

Table 1. Comparison of shortest interchain bonds in the Mikulski et al.<sup>21</sup> structure of  $\beta$  phase  $(SN)_x$  with the corresponding Van der Waals Radii.

Interchain Distances In  $(SN)_x$

Shortest Separation	Within (102) Plane	Between (102) Planes	V.D.W. (Å)
S-S	3.48	3.72	3.70
N-N	3.35	3.37	3.15
S-N	3.26	3.40	3.35

**END**

**FILMED**

**11-84**

**DTIC**